

1 **Mapping Global Non-Floodplain Wetlands**

2

3 Charles R. Lane¹, Ellen D’Amico², Jay R. Christensen^{3,*}, Heather E. Golden^{3,*}, Qiusheng Wu⁴, and
4 Adnan Rajib⁵

5

6 ¹ U.S. Environmental Protection Agency, Office of Research and Development, Center for Environmental
7 Measurement and Modeling, Athens, Georgia, United States of America

8 ² Pegasus Technical Service, Inc. c/o U.S. Environmental Protection Agency, Office of Research and
9 Development, Cincinnati, Ohio, United States of America

10 ³ U.S. Environmental Protection Agency, Office of Research and Development, Center for Environmental
11 Measurement and Modeling, Cincinnati, Ohio, United States of America

12 ⁴ Department of Geography & Sustainability, University of Tennessee, Knoxville, Tennessee, United
13 States of America

14 ⁵ Hydrology and Hydroinformatics Innovation Lab, Department of Civil Engineering, University of Texas
15 at Arlington, Arlington, Texas, United States of America

16

17 * These authors contributed equally to this work

18

19 **Correspondence:** Charles Lane (lane.charles@epa.gov) and Ellen D’Amico (damico.ellen@epa.gov)

20

21 **Abstract.** Non-floodplain wetlands – those located outside the floodplains – have emerged as integral
22 components to watershed resilience, contributing hydrologic and biogeochemical functions affecting
23 watershed-scale flooding extent, drought magnitude, and water-quality maintenance. However, the
24 absence of a global dataset of non-floodplain wetlands limits their necessary incorporation into water
25 quality and quantity management decisions and affects wetland-focused wildlife habitat conservation

26 outcomes. We addressed this critical need by developing a publicly available Global NFW (non-
27 floodplain wetland) dataset, comprised of a global river-floodplain map at 90 m resolution coupled with a
28 global ensemble wetland map incorporating multiple wetland-focused data layers. The floodplain,
29 wetland, and non-floodplain wetland spatial data developed here were successfully validated within 21
30 large and heterogenous basins across the conterminous United States. We identified nearly 33 million
31 potential non-floodplain wetlands with an estimated global extent of over 16 million km². Non-floodplain
32 wetland pixels comprised 53% of globally identified wetland pixels, meaning the majority of the globe's
33 wetlands likely occur external to river floodplains and coastal habitats. The identified Global NFWs were
34 typically small (median 0.039 km²), with a global median size ranging from 0.018-0.138 km². This novel
35 geospatial Global NFW static dataset advances wetland conservation and resource-management goals
36 while providing a foundation for global non-floodplain wetland functional assessments, facilitating non-
37 floodplain wetland inclusion in hydrological, biogeochemical, and biological model development. The
38 data are freely available through the United States Environmental Protection Agency's Environmental
39 Dataset Gateway (https://gaftp.epa.gov/EPADDataCommons/ORD/Global_NonFloodplain_Wetlands/) and
40 through <https://doi.org/10.23719/1528331> (Lane et al., 2023).

41

42 **1 Introduction**

43

44 Wetlands are recognized as globally important ecosystems providing functions leading to critical
45 provisioning (e.g., food, fresh water for domestic, agricultural, and industrial use) and regulating services
46 (e.g., flood and drought mitigation, water purification and waste treatment, and habitat; Millennium
47 Ecosystem Assessment, 2005). Despite their functional importance, wetlands are threatened worldwide by
48 myriad anthropogenic disturbances, including sea-level rise (IPCC, 2014), drainage and filling (Davidson
49 et al., 2014), water abstraction (Liu et al., 2017), consolidation (McCauley et al., 2015), invasive species
50 (Zedler and Kercher, 2004), and changing precipitation and temperature patterns (Winter, 2000). These
51 widespread and globally prevalent alterations to wetlands affect their functioning, resulting in increased

52 downgradient flooding (Golden et al., 2021), modified stream baseflows (Buttle, 2018), reduced pollution
53 mitigation (Evenson et al., 2018a), and habitat loss (Uden et al., 2015).

54

55 Watershed-scale wetland management is currently hampered by the paucity of accurate and fine-grained
56 maps of wetland location (Creed et al., 2017; Christensen et al., 2022). However, methods to identify
57 existing aquatic systems, including wetlands, that provide functions at global scales have recently
58 emerged, such as the Landsat-based 30 m global surface-water inundation data (Pekel et al., 2016), finer-
59 resolution satellite-based landcover maps (e.g., Zanaga et al., 2021), and groundwater-driven aquatic
60 system characterizations (Fan et al., 2013). In addition, methods utilizing digital elevation models to
61 identify topographic depressions likely to support aquatic systems with characteristic wetland features,
62 such as saturated soils and/or ponded waters, have also regionally proliferated (Wu et al., 2019a; Wu et
63 al., 2019b; Christensen et al., 2022).

64

65 These advancements in mapping wetland location, such as those located within the river floodplain or
66 geographically distal from floodplains, allow resource managers to better incorporate wetland
67 biogeochemical, hydrological, and biological functions and concomitantly ecosystem services into their
68 decision-making efforts. For instance, incorporating *floodplain* wetlands into decision-making advances
69 the wise management and conservation of mapped riparian ecosystems (Tullos, 2018; Kundzewicz et al.,
70 2018). Thus, recognizing the importance of wetlands located within active river floodplains, land-
71 management decisions are being made to quantify the functions and ecosystem services of these wetlands
72 and incorporate them into watershed-scale hydro-ecological decisions (e.g., Makungu and Hughes, 2021;
73 Rajib et al., 2021).

74

75 However, *non-floodplain wetlands* are typically not incorporated into watershed-scale conservation and
76 management planning (e.g., Sullivan et al., 2019), thereby ignoring their contributions to watershed-scale
77 resilience in response to biogeochemical and hydrological disturbances (Rains et al., 2016; Golden et al.,

78 2021; Lane et al., 2022). Non-floodplain wetlands are abundant inland freshwater wetlands located
79 distally from the floodplains of rivers and lakes (Lane and D'Amico, 2016; Lane et al., 2018). Though
80 typically small (Cohen et al., 2016), high biogeochemical processing rates within non-floodplain wetlands
81 have resulted in these systems being termed bioreactors (Marton et al., 2015). Indeed, a literature review
82 of over 600 articles found that the highest reactivity rates (pollutant mass removal per unit time) were
83 found in the smallest water bodies and wetlands (Cheng and Basu, 2017). Further, the high reactivity of
84 individual non-floodplain wetlands can cumulatively improve downgradient water quality conditions
85 (Golden et al., 2019; Evenson et al., 2021). Non-floodplain wetlands may therefore have an outsized
86 impact on a watershed's water quality.

87

88 Non-floodplain wetlands are also important ecosystems affecting water quantity (i.e., for storing and
89 gradually releasing water to downgradient rivers and streams). Specifically, precipitation is captured and
90 stored in non-floodplain wetlands prior to being discharged downgradient. During this storage period,
91 water can infiltrate to recharge aquifers, evaporate or transpire, or eventually “spill” overland and be
92 transported downstream (Jones et al., 2018; Buttle, 2018). These non-floodplain wetland water storage
93 functions attenuate storm flows (Shaw et al., 2012; Fossey and Rousseau, 2016; Blanchette et al., 2022)
94 and recharge groundwaters (Bam et al., 2020), thereby mitigating flood-hazards (Mclaughlin et al., 2014)
95 and ameliorating drought conditions by maintaining baseflow (Ameli and Creed, 2019).

96

97 Despite the important functions provided by non-floodplain wetlands (Biggs et al., 2017; Chen et al.,
98 2022) a substantive data gap remains: no global maps or datasets exist identifying the geospatial location
99 of non-floodplain wetlands and open waters. Regionally focused efforts, such as the recent work by Lane
100 and D'Amico (2016) and Lane et al. (2022) mapped the extent of non-floodplain wetlands (also known as
101 geographically isolated wetlands, Leibowitz, 2015; Mushet et al., 2015) across the geospatially data-rich
102 conterminous United States (CONUS, see abbreviation list in Appendix A). They found that 16-23 % of

103 freshwater systems were potential non-floodplain wetlands, suggesting a substantial yet hitherto unknown
104 portion of the globe's wetlands are likely also this vulnerable water resource.

105
106 Fortunately, geospatial data for identifying aquatic systems, including wetlands, are burgeoning. Global
107 land cover and land use geospatial datasets that include a wetland cover class continue to propagate (Hu
108 et al., 2017a), taking advantage of both lengthy time-series Landsat data (Homer et al., 2020) as well as
109 recently launched advanced high-resolution and/or synthetic aperture radar (SAR) equipped satellites
110 (e.g., Sentinel-1, Sentinel-2, plus many commercially available platforms; Martinis et al., 2022) and
111 topographic data sources and analyses (e.g., Wu et al., 2019b). Examples include the GlobeLand30 (Chen
112 et al., 2015), the European Space Agency (ESA) WorldCover 2020 (ESA, 2020), the Dynamic World
113 (Brown et al., 2022), as well as consortiums focusing on annual land cover change mapping (e.g.,
114 Tsendbazar et al., 2021). Several recent publications review the available wetland-focused datasets,
115 including Hu et al. (2017a, their Table 1), Davidson et al. (2018, their Table S1), Tootchi et al. (2019,
116 their Table 1), and Zhang et al. (2023, their Table 1). We summarize additional emerging global land
117 cover data sets related to surface water and wetlands in Appendix Table B1.

118
119 Lehner and Döll (2004) were amongst the first to publish a geospatially explicit global map focusing on
120 wetland extents. Their Global Lakes and Wetlands Database provides 1 km estimates of wetland
121 abundance. More recent and/or higher resolution wetland-focused datasets have emerged, including the 1
122 km global dataset from Hu et al. (2017b) that incorporates precipitation and a topographic wetness index,
123 and the multi-sourced 500 m composite maps of regularly flooded and groundwater-driven wetlands by
124 Tootchi et al. (2019). Tootchi et al.'s (2019) approach identified small and scattered wetlands. However,
125 they recognized the limitations inherent in their global product (ca. 500 m per pixel resolution) resulted in
126 omission errors for many wetland systems, especially those smaller than their 500 x 500 m (25 ha) data
127 resolution. This suggests, and Tootchi et al. (2019) acknowledged, that many (non-floodplain) wetlands
128 were omitted in the Tootchi et al. (2019) 500 m global product. Cohen et al. (2016) determined non-

129 floodplain wetlands in the CONUS are “unambiguously small”, e.g., their average non-floodplain wetland
130 area was just over two hectares (2.1 ha). Based on the “all or nothing” methodological approach in
131 Tootchi et al. (2019), > 12.5 ha of a given 25.0 ha cell [one homogenous pixel] would have to be
132 identified as wetland in their resampling of the finer-scale data – much larger than the average 2.1 ha
133 wetlands found in Cohen et al. (2016).

134
135 Concurrent with increasingly available global land cover and wetland data, there is an increasing global
136 focus on deriving floodplain and flood hazard-prone areal extents within river networks based on high-
137 resolution topographic data coupled with hydrologic and/or hydraulic modeling (Tullos, 2018;
138 Kundzewicz et al., 2018). The past decade has seen development of multiple regional to continental flood
139 models that span physically based approaches (e.g., 1-,2-, and 3-D hydrodynamic models) to empirical
140 models (including machine-learning approaches and statistical models) (see review by Mudashiru et al.
141 2021). On the global scale, openly accessible global flood models include those reviewed by Hoch and
142 Trigg (2019), namely CaMa-Flood (Yamazaki et al. 2011), GLOFRIS (Winsemius et al. 2013), JRC
143 (Dottori et al. 2016), CIMA-UNEP (Rudari et al. 2015), Fathom (Sampson et al. 2015), and ECMWF
144 (Papperberger et al. 2012). For instance, Sampson et al. (2015) created a global 90 m map of flood-prone
145 areas between 60° N and 56° S using a regional flood-frequency model. More recently, Nardi et al. (2019)
146 published a global floodplain dataset at 250 m resolution that extended from 60° N to 60° S developed
147 through a geomorphic or terrain-based analyses of floodplain elevations and maximum flood-prone areas
148 using a drainage-area scaling variable (Rajib et al. 2021). The evolution of the MERIT Hydro 90 m global
149 hydrography dataset by Yamazaki et al. (2019) and machine-learning approaches (e.g., Zhao et al. 2021)
150 has created additional opportunities to further advance the derivation of global floodplains, with improved
151 identification of flow accumulation area, river-basin shape, and river channel location.

152
153 These wetland-location and floodplain-extent data are critical for watershed-scale sustainable aquatic
154 resource policy decisions (Creed et al., 2017; Golden et al., 2017). The lack of these data can result in

155 disproportionately large model errors and potentially misguided management decisions when non-
156 floodplain wetlands are not incorporated in hydrological and biogeochemical models, ignoring their
157 watershed-scale impacts on flooding, drought, and water quality (Evenson et al., 2018a; Rajib et al., 2020;
158 Golden et al., 2021).

159

160 Here, we provide the first global geospatial dataset of non-floodplain wetlands. We incorporate the recent
161 development of a high-resolution global floodplain mapping algorithm based on digital terrain models by
162 Nardi et al. (2019). We couple these spatial floodplain data with higher-resolution modifications to the
163 gridded global wetland and open water data layers developed by Tootchi et al. (2019) that incorporate the
164 Pekel et al. (2016) satellite-based inundation product, modeled groundwater-driven wetland extent (Fan et
165 al. (2013), and ancillary satellite landcover data from Herold et al. (2015). We test the applicability of our
166 global dataset of non-floodplain wetlands in 21 large and spatial-data rich watersheds spanning nearly
167 700,000 km² across the CONUS. This novel global product identifying non-floodplain wetlands provides
168 for the quantification and estimation of the locations and extent of important aquatic systems with
169 abundant hydrological, biogeochemical, and biological functions, filling a noted research gap while
170 delivering useful data for informed natural resource decision-making and management (Creed et al.,
171 2017; Lane et al., 2022).

172

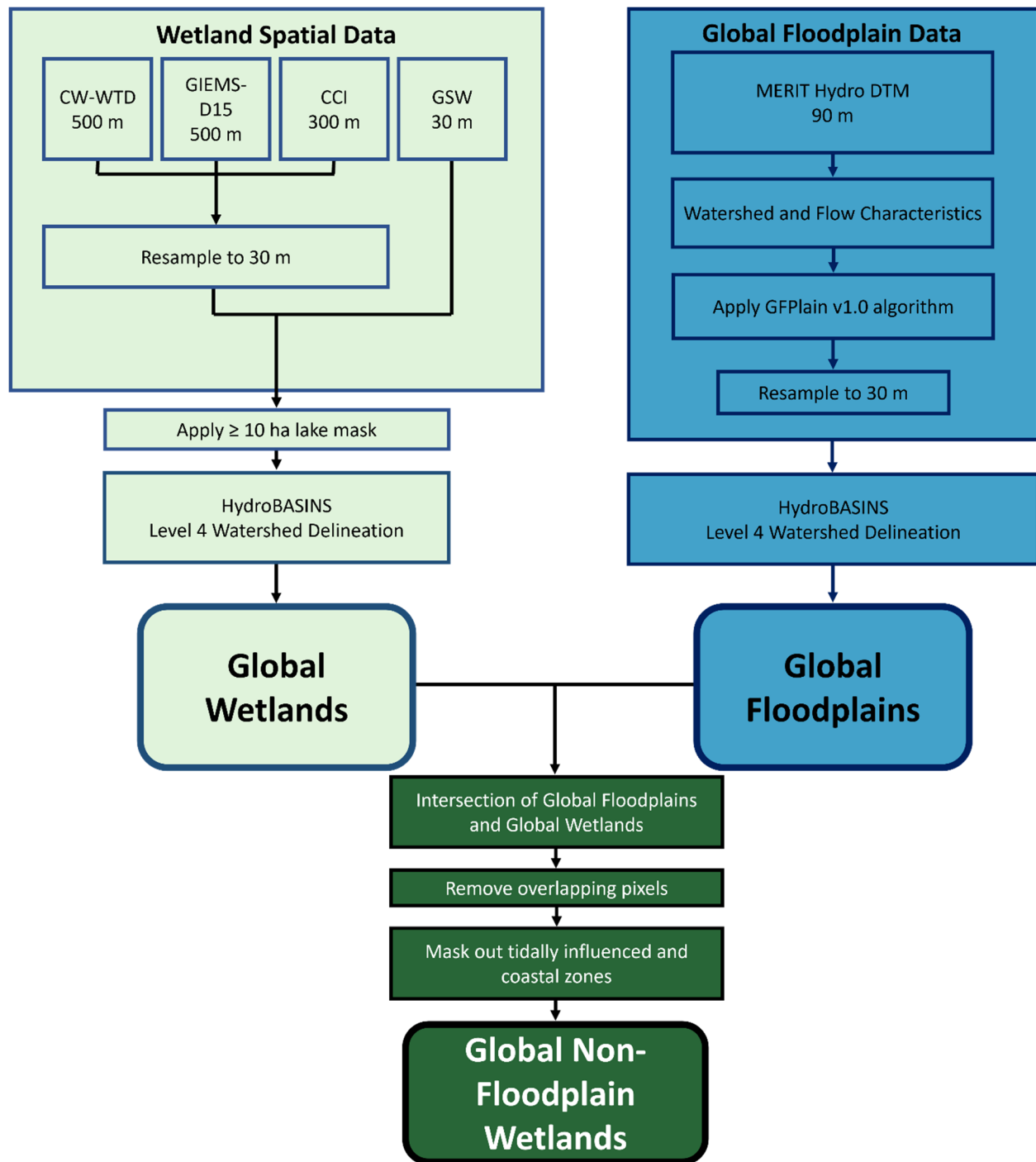
173 **2 Methodology and data**

174

175 Identifying global non-floodplain wetlands required the following steps: 1) determination of global
176 floodplain extent, 2) identification of the global distribution of wetlands, 3) spatial overlay (masking) of
177 floodplains and wetlands to derive a non-floodplain wetland data layer, and 4) data verification and
178 accuracy assessment. Steps 1-3 are outlined in a flow chart given in Fig. 1.

179

180



181
 182 **Figure 1.** Data flow chart identifying the main data sets and processes involved in deriving the Global Floodplain
 183 and Global Wetland data layers, as well as the intersection of those data to create the Global Non-floodplain
 184 Wetlands data product. Curved boxes represent final products, and abbreviations may be found in the text and
 185 Appendix A.

186 2.1 Global floodplain data

187

188 Nardi et al. (2019) combined space-borne elevation data and terrain analysis with a novel open-source
189 algorithm to delineate the geomorphic floodplains across the globe between 60° N and 60° S latitudes.
190 Conceptually, Nardi et al. (2019) identified floodplains from surrounding hillslopes as those low-lying
191 landscape features that have been naturally shaped by accumulated geomorphic effects of past flood
192 events. The original Nardi et al. (2019) dataset was limited in its spatial extent (60° N-60° S) and
193 resolution (250 m); this study sought to delineate global floodplain extent while concurrently identifying
194 floodplain features further up the river network than possible with 250 m pixels. Hence, we utilized the
195 freely available Nardi et al. (2019) GFPlain v1.0 algorithm and coupled this with the MERIT Hydro
196 (Multi-Error Removed Improved Terrain, Yamazaki et al., 2019), global raster digital terrain model data
197 to develop a higher resolution (90 m) geomorphic riverine floodplain for the globe, termed hereafter
198 GFPlain90.

199

200 The development of GFPlain90 required multiple steps. We first extracted elevation data from MERIT
201 Hydro and reprojected the data in UTM zones to prevent distortion when using the GFPlain algorithm.
202 We then developed the drainage network, drainage area, flow accumulation and flow direction data from
203 these data using the established scaling parameters in Nardi et al. (2019; power-law coefficient (a) of 0.01
204 and dimensionless exponent (b) = 0.30). We established 20 km² as the minimum contributing-area
205 threshold required to create the drainage network, balancing the development of a global stream-network
206 distribution and extent with computational requirements. We then globally organized the data by
207 HydroBASINS Level 4 basins (Lehner and Grill, 2013). HydroBASINS provides seamless watershed
208 boundaries and subbasin delineations at global scales; there are 1,342 Level 4 HydroBASINS globally.
209 The floodplain extent resolution of GFPlain90 was resampled (using nearest neighbor) to 30 m for
210 subsequent performance assessment and overlap analyses with the wetland spatial data. All spatial

211 analyses in this study were conducted using ArcGIS Pro v.2.9.x (ESRI, Redlands, California) and GRASS
212 GIS v 7.4.4 (OSGEO, Beaverton, Oregon).

213

214 **2.2 Global Wetland data**

215

216 Tootchi et al. (2019) developed a widely used composite global wetland map at ~500 m by combining
217 multiple data sources, including both satellite-based surface-water inundation mapping and vegetation
218 classification coupled with model-based approaches capturing important groundwater-driven wetland
219 systems. We specifically used the Tootchi et al. (2019) composite map consisting of both regularly
220 surface-water flooded wetlands (“regularly flooded wetlands,” RFWs) and groundwater discharge-
221 maintained wetlands (“groundwater-driven wetlands,” GDWs) as the foundation for our global wetland
222 map. Tootchi et al. (2019) merged the RFW and GDW maps, described below, to form a union product
223 used here that demonstrated a high correlation with available evaluation data, called the composite
224 wetland-water table depth (or CW-WTD).

225

226 **2.2.1 Original composite wetland data**

227

228 Regularly flooded wetlands (RFWs) derived by Tootchi et al. (2019) were based on three data sources: 30
229 m resolution Global Surface Water (GSW) by Pekel et al. (2016), 300 m Climate Change Initiative (CCI)
230 land cover data by Herold et al. (2015), and 500 m GIEMS-D15 wetland extent data by Fluet-Chouinard
231 et al. (2015). GSW data used by Tootchi et al. (2019) were developed from Landsat satellite imagery
232 analyses of pixels identified as inundated at least once during the 32-year period of record by Pekel et al.
233 (2016). CCI input wetland data for Tootchi et al. (2019) included both inundated and wetland vegetation-
234 classed pixels assessed during the period 2008-2012 by Herold et al. (2015). For GIEMS-D15, data
235 included were the mean annual maximum extent of pixels identified as wetlands using multi-sensor
236 satellite data by Prigent et al. (2007), downscaled to ~500 m resolution by Fluet-Chouinard et al. (2015).

237 GSW and CCI input data were resampled to ~500 m resolution using an “all or nothing” approach by
238 Tootchi et al. (2019). This means that a pixel categorization of “wetland” at 500 m resolution was given
239 by Tootchi et al. (2019) only if the majority of resampled finer-resolution input pixels were classed as
240 wetlands. The upward resampling from 30 m and 300 m to 500 m resulted in a loss of informative spatial
241 data on wetland extent from GSW and CCI. Tootchi et al. (2019) calculated that RFWs cover
242 approximately 9.7 % of the global land area (excluding lakes [sourced from (Messenger et al., 2016)],
243 Antarctica, and the Greenland ice sheet).

244
245 Groundwater-driven wetlands (GDWs in the analysis of Tootchi et al., 2019) used in this study were
246 based on the water-table depth estimates by Fan et al. (2013). Fan et al. (2013) developed a 1 km
247 resolution groundwater map based on climate and terrain variables that was validated by over 1 million
248 government-recorded and published observations. Fan et al. (2013) estimated that shallow groundwater
249 influenced nearly 15 % of groundwater-fed surface features, explaining important wetland patterning at
250 global scales (as well as vegetation classes at local and regional scales). A water-table depth threshold of
251 ≤ 20 cm was used by Tootchi et al. (2019) to identify groundwater-driven wetlands and they resampled
252 these data to ~500 m cell resolution. The GDW distribution based on water table depths covered
253 approximately 15 % of the global land mass (including large portions of the Amazon basin, coastal zones,
254 and North American and Siberian peatlands).

255
256 Tootchi et al. (2019) created a merged “final” product, called the composite wetland-water table depth
257 (CW-WTD) map, which is based on the union of the RFW and GDW maps. They measured an
258 approximately 3.8 % overlap between the total land pixels identified as wetlands in both the RFW and
259 GDW maps that comprise the CW-WTD, suggesting the different input maps capture different wetland
260 types. At the global scale, Tootchi et al. (2019) reported spatial Pearson correlations between CW-WTD
261 (wetland fractions at 3 arcmin, or ~4.9 km grids) and wetlands within GLWD (Lehner and Döll, 2004)

262 and Hu et al. (2017b) as $r=0.34$ and $r=0.43$, respectively. Tootchi et al. (2019, their Table 5 and S1)
263 provided additional analysis of the correlations between their global wetland product and existing
264 benchmark data. The total CW-WTD global wetland estimate was $\sim 21.1\%$ of the land mass, or
265 approximately 27.5 million km^2 (excluding large lakes, Antarctica, and the Greenland ice sheet; Tootchi
266 et al., 2019).

267

268 **2.2.2 Derived global wetland data**

269

270 To account for the acknowledged limitations of the Tootchi et al. (2019) data and to accurately identify
271 more of the existing small and, specifically, non-floodplain wetlands across the globe (e.g., those <25 ha),
272 we improved upon and augmented the CW-WTD (Tootchi et al., 2019) global wetland data layer with the
273 30 m native-resolution GSW (Pekel et al., 2016) and 300 m native-resolution CCI (Herold et al., 2015)
274 data. The inclusive wetland categories of Tootchi et al. (2019) were maintained, namely at least one
275 inundation event over a 32 year range (for GSW data) and CCI pixels defined as "...mixed classes of
276 flooded areas with tree covers, shrubs, or herbaceous covers plus inland water bodies..." (Tootchi et al.,
277 2019, p. 193). However, for our analysis we resampled the 500 m CW-WTD product to 30 m using the
278 nearest-neighbor approach and then added any identified wetland pixel from the CCI data (resampled
279 from 300 m to 30 m) and inundated pixel from the GSW data (30 m resolution). Resampling to a finer
280 resolution (as we did in our analysis) does not result in data losses: the same data are retained but are
281 divided into equal, smaller parts. However, moving from a finer resolution to coarser resolution (as in the
282 CW-WTD dataset's "all-or-nothing" approach) does cause data losses: fine-scale data are necessarily
283 aggregated (often by averaging) to a larger grid cell size, and therefore less information is retained. To
284 compensate for this data loss in the CW-WTD dataset, the finer resolution GSW (30 m) and CCI (300 m)
285 data were added back into the dataset. This resulted in a novel and encompassing wetland ensemble end-
286 product, hereafter termed the Global Wetlands dataset. This new dataset is inclusive of both finer-

287 resolution (30 m and 300 m) data, thereby accounting for a wide range of wetland sizes – such as smaller
288 non-floodplain wetlands (Cohen et al., 2016) – that remained unmapped by Tootchi et al. (2019).

289

290 **2.3 Global Non-Floodplain Wetlands (Global NFWs)**

291

292 To identify non-floodplain wetlands specifically, we overlaid our GFPlain90 floodplain data with our
293 mapped Global Wetlands data to mask wetland pixels collocated on the floodplain. Then, to avoid tidally
294 influenced wetlands, we conducted a region-group analysis to identify connected pixels abutting coastal
295 shorelines in order to mask wetlands in coastal areas (e.g., those directly abutting the shoreline and
296 spatially connected to tidally influenced areas). We used a four-directional contagion criterion to identify
297 connected pixels (i.e., those connected in cardinal directions). Subsequently, we applied a 1 km buffer to
298 the HydroBASINS (Lehner and Grill, 2013) coastline area and removed from our analyses any wetland
299 region-group partially or completely overlain by the 1 km coastline buffer. In addition, Tootchi et al.
300 (2019) removed lake systems (≥ 10 ha) from their wetland-focused data by masking aquatic layers using
301 HydroLAKES (Messenger et al., 2016). To avoid including large lakes in our emerging non-floodplain
302 wetland geospatial data, we also applied the HydroLAKES mask and removed lake systems ≥ 10 ha
303 (Messenger et al., 2016) from our Global Wetlands dataset. Thus, our final global non-floodplain wetland
304 data product (hereafter Global NFWs) did not include fluvial floodplain wetlands nor coastal wetland
305 complexes and large open water lacustrine (lake-like, Cowardin et al., 1979) systems.

306

307 **2.4 Data verification and assessment**

308

309 We evaluated the global products developed here through comparison of high-resolution floodplain and
310 wetland extent data from 21 basins representing disparate climatic (according to the Köppen-Geiger
311 classification, Beck et al., 2018), elevation, and land-use gradients within the CONUS (Fig. 2;

312 summarized in Table B2). We specifically focused on the CONUS for product assessment because of its
313 wide-ranging data availability and diversity of physiographic and climatic regions.

314

315 **2.4.1 Verifying floodplain extent**

316

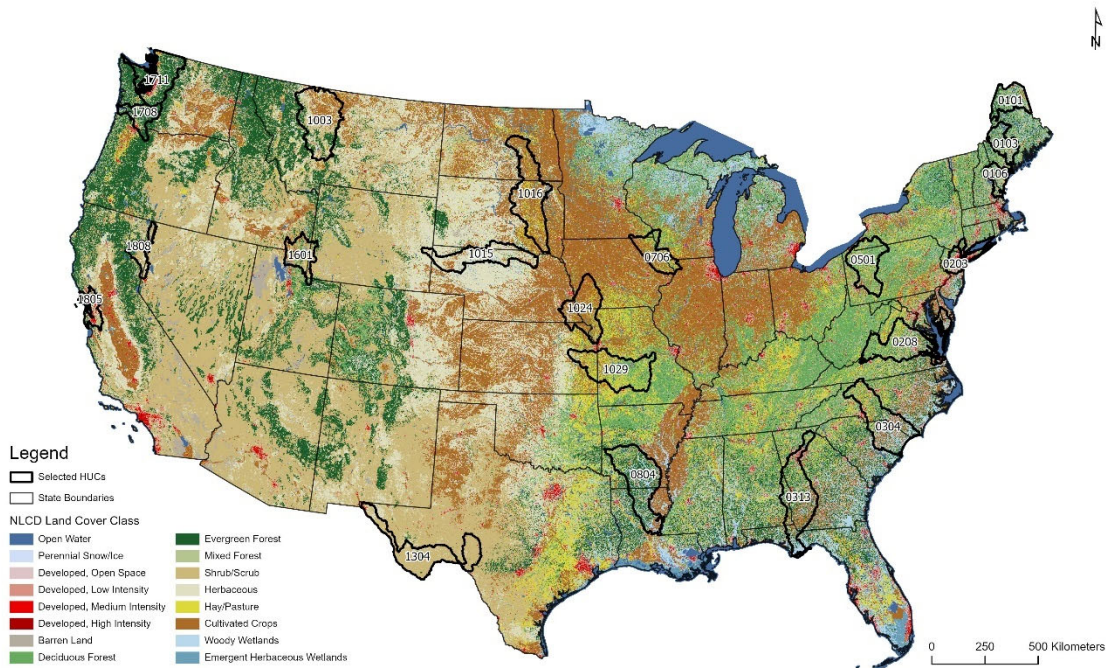
317 We used a recently developed machine learning (ML)-based 30 m resolution CONUS floodplain dataset
318 (Woznicki et al., 2019) as the benchmark to evaluate our GFPlain90 global floodplain data. Specifically,
319 the ML model by Woznicki et al. (2019) used the U.S. Federal Emergency Management Agency (FEMA)
320 100 yr floodplain (i.e., a 1 % chance of coastal or fluvial flood-inundation in a given year; Jakubínský et
321 al., 2021) as the training data, and subsequently used soil and topographic characteristic along with land
322 cover to identify potential floodplain grid cells across CONUS at 30 m resolution. Woznicki et al. (2019)
323 reported that their ML approach correctly identified ~79 % of the FEMA 100 yr coastal and fluvial
324 floodplains, providing spatially complete 100 yr floodplain coverage totaling 980,450 km² across the
325 CONUS.

326

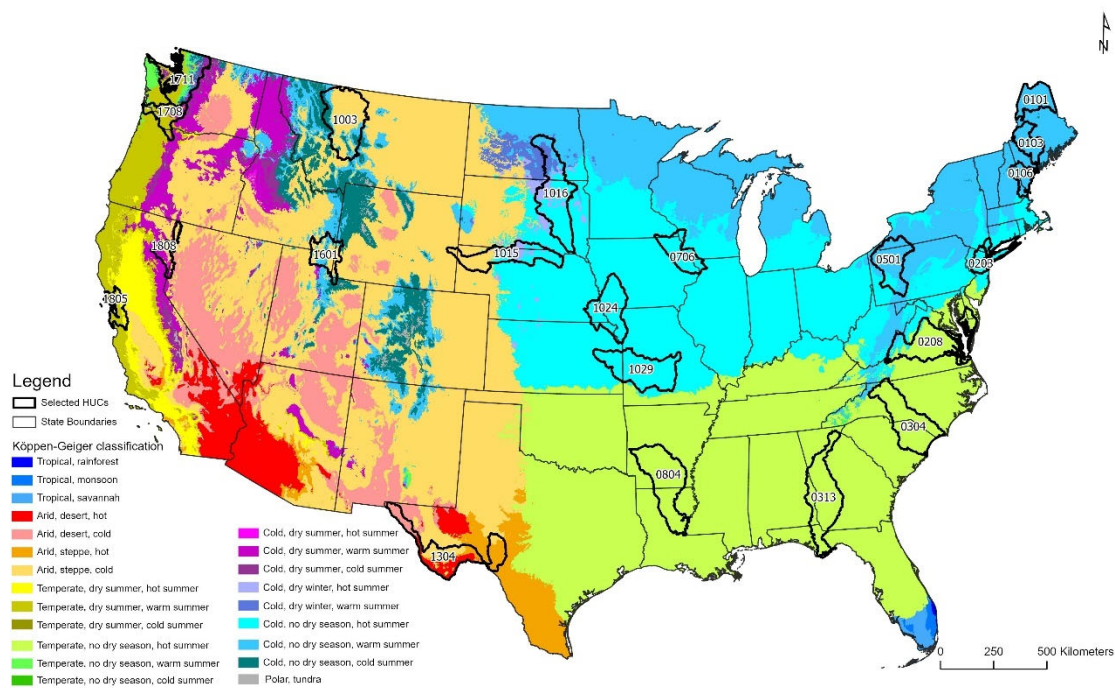
327 **2.4.2 Verifying wetland and non-floodplain wetland extent**

328

329 We evaluated our inclusive Global Wetlands and Global NFWs datasets in 21 basins covering ~680,000
330 km² (Fig. 2). We contrasted our products to the 2016 National Land Cover Database (NLCD, Dewitz,
331 2019). The NLCD is a 30 m Landsat satellite-based geospatial product with an overall accuracy of 86 %
332 that incorporates high-resolution aerial imagery of wetland location for model parameterization and
333 calibration (Jin et al., 2019; Wickham et al., 2021). Three NLCD classes were selected for comparison
334 with the Global Wetland product: woody wetlands, emergent herbaceous wetlands, and open water. To



335



336

337 **Figure 2.** Twenty-one validation watersheds were selected from across CONUS to capture the breadth and extent of
 338 land use (top, NLCD 2019) and climate and physiographic regions (bottom) within CONUS according to the
 339 Köppen-Geiger classification (Beck et al., 2018); also summarized in Table B2). The Hydrologic Unit Code (HUC)
 340 classifications are sourced from USGS Watershed Boundary Dataset (2022).

341
 342 assess the relative improvement of our 30 m Global Wetlands and Global NFWs dataset with the 500 m
 343 Tootchi et al. (2019) data, we also contrasted the CW-WTD with the NLCD classes within the
 344 verification watersheds. For equal comparisons, following Tootchi et al. (2019) we used the Messenger et
 345 al. (2016) HydroLAKES to mask out large lake systems (≥ 10 ha) from both the Global Wetlands and the
 346 NLCD data within the 21 verification watersheds.

347

348 **2.4.3 Standard performance measures**

349

350 We evaluated the floodplain and wetland spatial data within the 21 validation watersheds using
 351 commonly employed performance measures. Following Wing et al. (2017), we first created a contingency
 352 table for our performance assessment (Table 1). As noted, we selected 20 km² as the minimum
 353 contributing area to develop stream networks in our global floodplain analysis, a reasonable area for flow-
 354 accumulation that balances computational efficiency for global geospatial model development. Woznicki
 355 et al. (2019), our benchmark floodplain dataset, used a 4.5 km² contributing area in their high-resolution
 356

357 **Table 1.** Contingency table of possible outcomes for each cell used in assessing the performance of either the
 358 floodplain or wetland geospatially modeled data. We contrasted published benchmark data from Woznicki et al.
 359 (2019) for floodplain extent against modeled GFPlain90 data. Wetland comparisons contrasted NLCD wetlands
 360 (Dewitz, 2019, open water and wetland classes) against both Global Wetlands and Global NFWs data. Table is
 361 modified from Wing et al. (2017). The subscript “1” equates to a positive outcome or overlapping extent for either
 362 the modeled (M) or benchmark (B) data whereas a zero means no data overlap or a negative outcome.

	Floodplain [or Wetland] in Benchmark data	Not Floodplain [or Wetland] in Benchmark data
Floodplain [or Wetland] in Modeled data	M ₁ B ₁	M ₁ B ₀
Not Floodplain [or Wetland] in Modeled data	M ₀ B ₁	M ₀ B ₀

363

364 CONUS analysis. To appropriately compare between datasets of two varying resolutions, we removed
365 stream and river network components from the Woznicki et al. (2019) validation dataset developed with
366 contributing areas $<20 \text{ km}^2$, as our model did not discern landscape data at that granularity.

367
368 To provide a full assessment of our geospatial modeling performance, we contrasted our GFPlain90
369 floodplain dataset across the 21 validation watersheds using the approaches described below following
370 Sampson et al. (2015), Wing et al. (2017), and others (e.g., Bates and De Roo, 2000; Alfieri et al., 2014;
371 Sangwan and Merwade, 2015; Jafarzadegan et al., 2018; Woznicki et al., 2019). We first contrasted our
372 GFPlain90 floodplains to Woznicki et al. (2019), our benchmark floodplain data. We then analyzed the
373 watershed-scale comparison of our Global Wetlands product versus the NLCD wetlands (combined open
374 water and wetland classes), our benchmark wetlands data. We followed with a comparison focusing only
375 on our Global NFWs data and those NLCD wetlands and open water pixels that were determined to be
376 non-floodplain systems (i.e., NLCD data that also do not overlap the GFPlain90 data nor coastal waters
377 and with lakes $>10 \text{ ha}$ removed). These NLCD wetlands were our benchmark non-floodplain wetland
378 data. Lastly, we assessed the mean and aggregate error bias of our analyses by exploring results at coarser
379 spatial granularity (i.e., 1 km pixel size) along the riverine network (for floodplain assessment) and, for
380 wetland metrics, throughout the entirety of our 21 performance assessment watersheds (Sampson et al.,
381 2015; Wing et al., 2017). The metrics described below and in Table 2 were used in our analyses.

382
383 *Hit Rate* (Bates and De Roo, 2000; Horritt and Bates, 2002; Tayefi et al., 2007) also referred to as Recall
384 (Woznicki et al., 2019) and Correct (Sangwan and Merwade, 2015), measures how well a geospatial
385 model classification replicates the benchmark data but does not penalize for overprediction. *H* varies from
386 0, where there is no overlap between the modeled data and the benchmark data, to 1 where the modeled
387 data completely contain the benchmark data. *Precision* (Woznicki et al., 2019), also known as Spatial
388 Coincidence (Tootchi et al., 2019), indicates the proportion of the benchmark data that are correctly
389 predicted and mapped in the modeled data. This metric, *P*, also ranges from 0 to 1 with higher values

390 **Table 2.** Performance metrics used in validation assessments of floodplain and wetland data layers. Data for
 391 assessment (e.g., M_1B_1) follow that given in Table 1 and modified from Wing et al. (2017), with the exception of
 392 equations 7 and 8 (see text).

Equation Number	Metrics	Equation	Range
1	Hit Rate (H)	$Hit\ Rate\ (H) = \frac{M_1B_1}{M_1B_1 + M_0B_1}$	0 - 1, higher is “better”
2	Precision (P)	$Precision\ (P) = \frac{M_1B_1}{M_1B_1 + M_1B_0}$	0 - 1, higher is “better”
3	False Alarm Ratio (FA)	$False\ Alarm\ Ratio\ (FA) = \frac{M_1B_0}{M_1B_0 + M_1B_1}$	0 - 1, lower is “better”
4	Critical Success Index (CSI)	$Critical\ Success\ Index\ (CSI) = \frac{M_1B_1}{M_1B_1 + M_0B_1 + M_1B_0}$	0 - 1, higher is “better”
5	F1	$F1 = 2 \left(\frac{H \times P}{H + P} \right)$	0 - 1, higher is “better”
6	Error Bias (EB)	$Error\ Bias\ (EB) = \frac{M_1B_0}{M_0B_1}$	0 - ∞; <1 underprediction, 1 = no bias, >1 indicate overprediction
7	Mean Absolute Error (EA)	$Mean\ Absolute\ Error\ (EA) = \frac{\sum_{i=1}^N M-B }{N}$	0 - 1, lower is “better”
8	Aggregate Error Bias (BA)	$Aggregate\ Error\ Bias\ (BA) = \frac{\sum_{i=1}^N M-B}{N}$	-1 to 1, negative values indicate underprediction, positive values overprediction

393
 394 indicating better performance. The *False Alarm Ratio* (Sampson et al., 2015; Wing et al., 2017) also
 395 known as the False Discovery Ratio, quantifies modeled data overprediction relative to the benchmark
 396 data. *F* varies from 0 (zero false alarms) to 1 (all false alarms); lower values are considered better
 397 performance. The False Alarm Ratio can also be calculated as 1 - *Precision* (Woznicki et al., 2019). The
 398 *Critical Success Index* (CSI, Bates and De Roo, 2000; Aronica et al., 2002; Werner et al., 2005; Fewtrell
 399 et al., 2008), also known as Jaccard’s Index (Tootchi et al., 2019), and Fit (Sangwan and Merwade, 2015),
 400 penalizes for both over- and under-prediction, ranging from 0 (no match) to 1 (perfect match). Woznicki
 401 et al. (2019) utilized a performance metric, *F1*, which combines the *Hit Rate* (called Recall by Woznicki
 402 et al. 2019) and *Precision* using their harmonic mean. *F1* also varies from 0 to 1, with higher values
 403 indicating better performance. *Error Bias* (*EB*) characterizes the tendency of the model towards under- or

404 over-prediction (Sampson et al., 2015). Values of 1 indicate no bias, $0 \leq EB < 1$ indicates underprediction
405 whereas $1 < EB \leq \infty$ indicates the model is tending towards overprediction.

406
407 Lastly, two additional metrics were calculated that assessed performance at the 30 arc-sec (~1 km) scale.
408 These measures, *Mean Absolute Error* and *Aggregate Error Bias* (Sampson et al., 2015; Wing et al.,
409 2017), characterize the data accuracy across large spatial extents. Large spatial extents are areas where 30
410 m data and overlap accuracy is less a concern than general dataset performance for broad-scale end-user
411 applications (e.g., when coarser, watershed-scale “lumped” hydrologic characterizations of water storage
412 are all that is required). For these metrics, both estimated and benchmark data were resampled to 1 km
413 resolution across the whole of each watershed; values within each 1 km pixel ranged from 0 to 1 and
414 represented the fraction of the 30 m resolution estimates and benchmark data. We assessed floodplain
415 estimates after calculating the fractional abundance comprising each 1 km² pixel within a 1 km buffer
416 around the Woznicki et al. (2019) floodplain data. We additionally analyzed all wetlands at the
417 watershed-scale as well as focusing on non-floodplain wetlands (e.g., wetlands exclusive of the
418 GFPlain90 floodplain or coastal connections, our target aquatic system). In Eq. 7 and 8 (given in Table 2),
419 M is the area estimated as floodplain (or wetland), B is the benchmark floodplain (or wetland) area, and N
420 is the number of 1 km cells with data. *Mean Absolute Error* and *Aggregate Error Bias* were calculated for
421 each of the 21 HUCs, following Wing et al. (2017).

422

423 **3 Results**

424

425 **3.1 Floodplain data performance**

426

427 The GFPlain90 floodplain data (Fig. 3) performed well when contrasted with the 100 yr coastal and
428 fluvial floodplain extent data from Woznicki et al. (2019), even though our analyses do not map coastal
429 floodplains. A median Hit Rate of 0.77 suggests that nearly 80% of the benchmark floodplain from

430 Woznicki et al. (2019) was similarly captured by the GFPlain90 floodplain data (see Appendix Table B3).
431 In addition, the median False Alarm of 0.26 indicates that for every three pixels correctly identified as
432 within the Woznicki et al. (2019) floodplain, one pixel was incorrectly identified as such (i.e., a
433 commission error measure); this is evident in wider GFPlain90 floodplains in lower river reaches than
434 predicted by Woznicki et al. (2019). These performance values are similar to those reported by Woznicki
435 et al. (2019, False Alarm 0.22) and Wing et al. (2017, False Alarm 0.34-0.37). Critical Success Index
436 (CSI) scores penalize for over-prediction; our median value of 0.53 approximates previously published
437 regional (e.g., Sangwan and Merwade, 2015, CSI values ranging from 0.44-0.89) and continental flood-
438 extent approaches (e.g., Sampson et al., 2015, CSI values from 0.43-0.67; Wing et al., 2017; CSI values
439 between 0.50 and 0.55 reported). Median Precision (0.74) and F1 (0.70) values approximate those in the
440 literature as well (e.g., Woznicki et al., 2017 reported values of 0.78 for both). Median Error Bias values
441 of 1.0 suggests the model neither over-estimates nor under-estimates floodplain extents (Wing et al.
442 2017). Mean Absolute Error of 0.08 reported here indicates an approximate 8 % difference between our
443 GFPlain90 model and that of Woznicki et al. (2017) at the 1 km cell resolution.

444

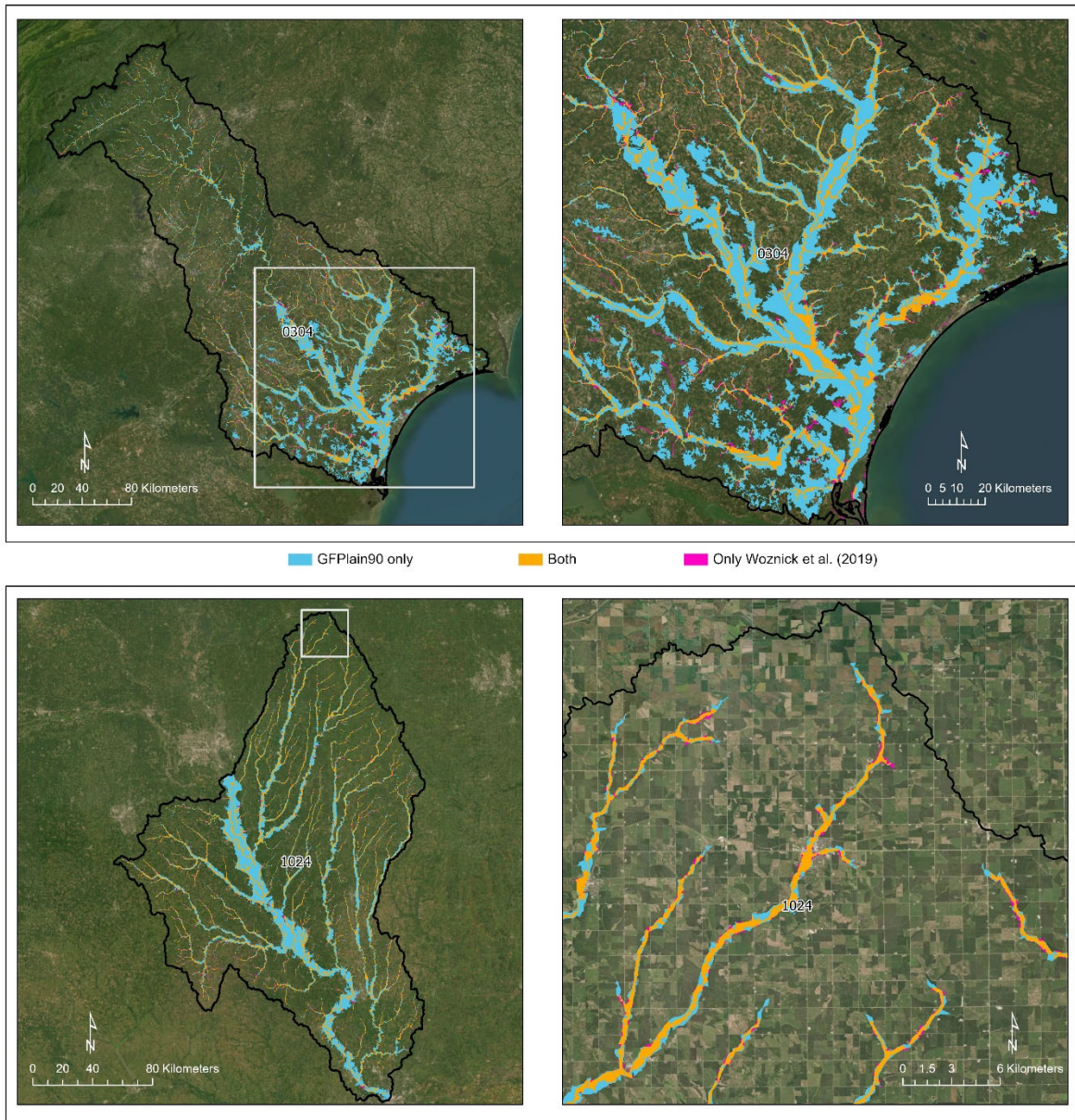
445 **3.2 Wetland data performance**

446

447 **3.2.1 Global Wetland dataset**

448

449 The novel ensemble Global Wetlands approach improved upon the previously published Tootchi et al.
450 (2019) research product, the CW-WTD (Table 3) when contrasted with CONUS data. A median Hit Rate
451 value of 0.24 indicates that both the inclusive Global Wetlands and CW-WTD captured ~one-quarter of
452 the high-resolution, 30-m pixel size NLCD wetlands and open waters in the validation dataset. However,
453 across the 21 validation watersheds the Global Wetlands dataset developed here correctly identified more
454



455
 456 **Figure 3.** The robust performance of GFPlain90 relative to the benchmark Woznicki et al. (2019) floodplain data is
 457 evident in the two rows, with the top panels (HUC_0304) different spatial extents of a coastal watershed spanning
 458 North and South Carolina, USA, and the bottom two panels different spatial extents of a Midwestern USA
 459 watershed (HUC_1024). The mainstem of the river network appeared wider in the GFPlain90 data in both examples,
 460 especially in the lower reaches, though the complete network was well represented (i.e., floodplains were identified
 461 to the furthest extent of the stream network’s headwaters). Satellite imagery is sourced from ESRI (2022).

462 wetlands than the CW-WTD alone, as indicated by an 8% mean increase in Precision, 43 % increase in
463 Critical Success Index, 38 % increase in F1, a -8 % decrease in the False Alarm ratio, and a 21 %
464 decrease in Error Bias. At coarser, 1 km² scales, there was a slight decrease in the Mean Absolute Error
465 associated with the Global Wetlands, and no difference in Aggregate Error Bias between the data
466 products.

467

468 **3.2.2 Global Non-Floodplain Wetland (Global NFW) dataset**

469

470 Non-floodplain wetland identification using the Global Wetlands data (i.e., Global NFWs) similarly
471 improved upon the CW-WTD product (Fig. 4). For instance, though the Hit Rate values were low (e.g.,
472 median values ≤ 0.10), underscoring both the difficulty in mapping non-floodplain wetlands and the
473 challenge of assessing performance using high-resolution data, Global NFW analyses correctly identified
474 50 % more non-floodplain wetlands than the CW-WTD (Table 4, Tootchi et al., 2019). Improvements
475 when focusing on non-floodplain wetlands were found in every category with the Global NFWs dataset,
476 demonstrating increased non-floodplain wetland accuracy versus the original CW-WTD across the
477 median metric values for Precision, Critical Success Index, F1, False Alarms, and Error Bias (e.g., 33 %
478 increase in Precision, 20 % increase in Critical Success Index, 10 % increase in F1 scores, and a 12 %
479 decrease in False Alarms and a 19 % decrease in Error Bias). There was no difference between the
480 datasets with median values for Mean Absolute Error (median values for both = 0.09) or Aggregate Error
481 Bias (median values for both = 0.07). Thus, at the 1 km² cell size, there was <10 % difference between
482 both the CW-WTD and the Global NFWs and the benchmark NLCD non-floodplain wetlands and open
483 waters (with the difference mostly stemming from an increase in identified wetlands with both CW-WTD
484 and Global NFWs, as indicated with the positive Aggregate Error Bias values).

485

486

487

488
 489
 490
 491
 492
 493
 494
 495

Table 3. Spatial performance assessment of both the Global Wetland (abbreviated here as GW) and CW-WTD (abbreviated here as WTD, Tootchi et al., 2019) datasets when contrasted with the benchmark NLCD wetlands (Dewitz, 2019). The first six equations directly assess the spatial concordance and overlap between each spatial dataset and the benchmark (e.g., CW-WTD contrasted with the NLCD), whereas Mean Absolute Error (MAE, Eq. 7) and Aggregate Error Bias (AEB, Eq. 8) are coarser fractional analyses measured throughout each watershed (e.g., the proportional abundance NLCD within each 1 km² cell is contrasted with the proportional abundance of Global Wetlands predicted correctly within that cell).

Hydrologic Unit Code (HUC) ID	Hit Rate		Precision		False Alarm		Critical Success	
	(Eq. 1)		(Eq. 2)		(Eq. 3)		(Eq. 4)	
	WTD	GW	WTD	GW	WTD	GW	WTD	GW
HUC_0101	0.31	0.32	0.51	0.53	0.49	0.47	0.24	0.25
HUC_0103	0.26	0.28	0.42	0.45	0.58	0.55	0.19	0.21
HUC_0106	0.25	0.27	0.41	0.44	0.59	0.56	0.18	0.20
HUC_0203	0.12	0.12	0.51	0.53	0.49	0.47	0.11	0.11
HUC_0208	0.31	0.33	0.56	0.65	0.44	0.35	0.25	0.28
HUC_0304	0.42	0.43	0.65	0.69	0.35	0.31	0.35	0.36
HUC_0313	0.39	0.41	0.58	0.64	0.42	0.36	0.30	0.33
HUC_0501	0.15	0.17	0.57	0.64	0.43	0.36	0.14	0.15
HUC_0706	0.24	0.25	0.86	0.92	0.14	0.08	0.23	0.24
HUC_0804	0.45	0.46	0.70	0.75	0.30	0.25	0.38	0.40
HUC_1003	0.14	0.16	0.32	0.41	0.68	0.59	0.11	0.13
HUC_1015	0.25	0.40	0.17	0.42	0.83	0.58	0.12	0.26
HUC_1016	0.13	0.16	0.54	0.70	0.46	0.30	0.12	0.15
HUC_1024	0.10	0.10	0.67	0.75	0.33	0.25	0.09	0.10
HUC_1029	0.10	0.13	0.51	0.72	0.49	0.28	0.09	0.13
HUC_1304	0.02	0.02	0.44	0.52	0.56	0.48	0.02	0.02
HUC_1601	0.29	0.33	0.34	0.45	0.66	0.55	0.19	0.24
HUC_1708	0.24	0.24	0.48	0.49	0.52	0.51	0.19	0.20
HUC_1711	0.09	0.10	0.46	0.51	0.54	0.49	0.08	0.09
HUC_1805	0.14	0.15	0.62	0.64	0.38	0.36	0.13	0.13
HUC_1808	0.12	0.13	0.51	0.55	0.49	0.45	0.11	0.11
Median	0.24	0.24	0.51	0.55	0.49	0.45	0.14	0.20
Difference		0.00		0.04		-0.04		0.06
Change (%)		0.0		7.8		-8.2		42.9

496

497 **Table 3.** (Continued)

Hydrologic Unit Code (HUC) ID	F1		Error Bias		MAE		AEB	
	(Eq. 5)		(Eq. 6)		(Eq. 7)		(Eq. 8)	
	WTD	GW	WTD	GW	WTD	GW	WTD	GW
HUC_0101	0.38	0.40	0.43	0.40	0.18	0.17	0.09	0.09
HUC_0103	0.32	0.34	0.50	0.47	0.16	0.15	0.06	0.07
HUC_0106	0.31	0.33	0.49	0.46	0.20	0.19	0.08	0.08
HUC_0203	0.19	0.20	0.13	0.13	0.36	0.36	0.28	0.28
HUC_0208	0.40	0.44	0.35	0.27	0.17	0.17	0.09	0.10
HUC_0304	0.51	0.53	0.39	0.34	0.21	0.21	0.12	0.13
HUC_0313	0.47	0.50	0.48	0.38	0.16	0.16	0.07	0.09
HUC_0501	0.24	0.26	0.14	0.11	0.10	0.10	0.09	0.09
HUC_0706	0.37	0.39	0.05	0.03	0.12	0.12	0.11	0.12
HUC_0804	0.55	0.57	0.36	0.29	0.20	0.20	0.12	0.14
HUC_1003	0.19	0.23	0.34	0.27	0.04	0.04	0.02	0.02
HUC_1015	0.21	0.41	1.59	0.91	0.05	0.04	-0.01	0.00
HUC_1016	0.21	0.26	0.13	0.08	0.26	0.26	0.23	0.24
HUC_1024	0.17	0.18	0.05	0.04	0.14	0.14	0.13	0.14
HUC_1029	0.17	0.22	0.11	0.06	0.11	0.12	0.10	0.11
HUC_1304	0.04	0.04	0.02	0.02	0.08	0.08	0.08	0.08
HUC_1601	0.31	0.38	0.80	0.59	0.05	0.05	0.01	0.01
HUC_1708	0.32	0.33	0.34	0.33	0.15	0.15	0.08	0.08
HUC_1711	0.15	0.17	0.12	0.11	0.17	0.17	0.14	0.15
HUC_1805	0.23	0.24	0.10	0.10	0.25	0.26	0.21	0.21
HUC_1808	0.20	0.20	0.13	0.12	0.09	0.09	0.07	0.07
Median	0.24	0.33	0.34	0.27	0.16	0.15	0.09	0.09
Difference		0.09		0.07		-0.01		0.00
Change (%)		37.5		-20.6		-6.3		0.0

498

499

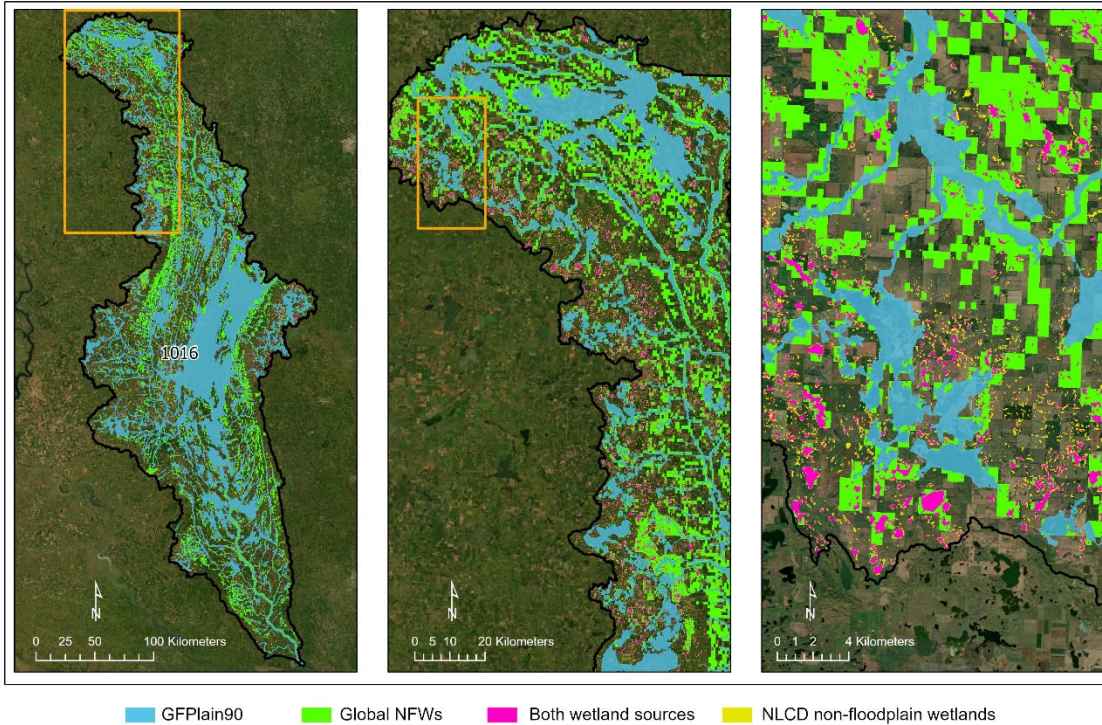


Figure 4. Demonstration of the relative accuracy of the Global NFWs in identifying non-floodplain wetlands using a Prairie Pothole Region watershed (HUC_1016, see Fig. 2) replete with abundant non-floodplain wetlands. Correctly identified wetlands occur in both wetland sources (magenta color). Omission errors (NLCD non-floodplain wetlands, smaller systems in yellow) and commission errors (Global NFWs, green) are evident as a result of the higher resolution of the NLCD validation dataset. Satellite imagery sourced from ESRI (2022). Note the scale increasing from left panel to right panel (i.e., the orange box in the first panel is shown in the second panel at a higher resolution, and the box in the second panel is shown in the last panel at an even higher resolution).

508 **Table 4.** Non-floodplain wetland performance metrics contrasting both the Global NFWs (abbreviated here as
509 GNFW) and CW-WTD (abbreviated here as WTD, Tootchi et al., 2019) non-floodplain wetland spatial data with the
510 benchmark NLCD wetlands (Dewitz, 2019). Descriptions of the metrics are the same as in Table 3, though the focus
511 here is on wetlands outside the GFPlain90-derived floodplain.

Hydrologic Unit Code (HUC) ID	Hit Rate		Precision		False Alarm		Critical Success Index	
	(Eq. 1)		(Eq. 2)		(Eq. 3)		(Eq. 4)	
	WTD	GNFW	WTD	GNFW	WTD	GNFW	WTD	GNFW
HUC_0101	0.24	0.25	0.43	0.45	0.57	0.55	0.18	0.19
HUC_0103	0.17	0.18	0.30	0.32	0.70	0.68	0.12	0.13
HUC_0106	0.15	0.18	0.14	0.17	0.86	0.83	0.08	0.10
HUC_0203	0.12	0.13	0.20	0.23	0.80	0.77	0.08	0.09
HUC_0208	0.14	0.16	0.34	0.41	0.66	0.59	0.11	0.13
HUC_0304	0.26	0.28	0.45	0.49	0.55	0.51	0.20	0.21
HUC_0313	0.21	0.23	0.35	0.40	0.65	0.60	0.15	0.17
HUC_0501	0.05	0.07	0.32	0.41	0.68	0.59	0.05	0.06
HUC_0706	0.05	0.06	0.63	0.72	0.37	0.28	0.05	0.05
HUC_0804	0.30	0.31	0.51	0.55	0.49	0.45	0.23	0.25
HUC_1003	0.04	0.07	0.13	0.21	0.87	0.79	0.03	0.05
HUC_1015	0.07	0.25	0.05	0.28	0.95	0.72	0.03	0.15
HUC_1016	0.07	0.11	0.31	0.53	0.69	0.47	0.06	0.10
HUC_1024	0.02	0.04	0.18	0.41	0.82	0.59	0.02	0.04
HUC_1029	0.03	0.06	0.25	0.58	0.75	0.42	0.03	0.06
HUC_1304	0.00	0.00	0.26	0.33	0.74	0.67	0.00	0.00
HUC_1601	0.05	0.09	0.07	0.16	0.93	0.84	0.03	0.06
HUC_1708	0.06	0.06	0.33	0.35	0.67	0.65	0.05	0.05
HUC_1711	0.04	0.05	0.22	0.27	0.78	0.73	0.04	0.05
HUC_1805	0.06	0.07	0.27	0.30	0.73	0.70	0.05	0.06
HUC_1808	0.05	0.06	0.25	0.36	0.75	0.64	0.04	0.06
Median	0.06	0.09	0.27	0.36	0.73	0.64	0.05	0.06
Difference		0.03		0.09		-0.09		0.01
Change (%)		50.0		33.3		-12.3		20.0

512

513

514 **Table 4.** (Continued)

Hydrologic Unit Code (HUC) ID	F1		Error Bias		Mean Absolute Error		Aggregate Error Bias	
	(Eq. 5)		(Eq. 6)		(Eq. 7)		(Eq. 8)	
	WTD	GFW	WTD	GFW	WTD	GFW	WTD	GFW
HUC_0101	0.31	0.32	0.41	0.39	0.16	0.16	0.08	0.09
HUC_0103	0.21	0.23	0.48	0.46	0.14	0.14	0.06	0.06
HUC_0106	0.14	0.18	1.11	1.03	0.11	0.11	-0.01	0.00
HUC_0203	0.15	0.17	0.53	0.51	0.09	0.09	0.03	0.03
HUC_0208	0.20	0.23	0.32	0.28	0.10	0.10	0.07	0.07
HUC_0304	0.33	0.35	0.44	0.40	0.17	0.17	0.08	0.09
HUC_0313	0.27	0.29	0.51	0.45	0.12	0.12	0.05	0.06
HUC_0501	0.09	0.11	0.12	0.10	0.09	0.09	0.07	0.08
HUC_0706	0.09	0.10	0.03	0.02	0.09	0.09	0.09	0.09
HUC_0804	0.38	0.40	0.43	0.37	0.13	0.13	0.07	0.07
HUC_1003	0.07	0.10	0.32	0.26	0.02	0.03	0.01	0.01
HUC_1015	0.06	0.26	1.46	0.85	0.03	0.02	-0.01	0.00
HUC_1016	0.11	0.19	0.17	0.11	0.15	0.15	0.12	0.13
HUC_1024	0.03	0.07	0.09	0.06	0.05	0.05	0.04	0.05
HUC_1029	0.05	0.11	0.09	0.05	0.08	0.08	0.07	0.07
HUC_1304	0.00	0.01	0.01	0.01	0.06	0.06	0.05	0.06
HUC_1601	0.05	0.11	0.68	0.50	0.02	0.02	0.00	0.01
HUC_1708	0.10	0.10	0.12	0.12	0.11	0.11	0.09	0.10
HUC_1711	0.07	0.09	0.16	0.15	0.09	0.09	0.07	0.07
HUC_1805	0.10	0.11	0.18	0.17	0.10	0.10	0.07	0.07
HUC_1808	0.08	0.11	0.15	0.12	0.02	0.02	0.01	0.01
Median	0.10	0.11	0.32	0.26	0.09	0.09	0.07	0.07
Difference		0.01		-0.06		0.00		0.00
Change (%)		10.0		-18.8		0.0		0.0

515

516

517 **3.3 Global extent analyses and synthesis**

518

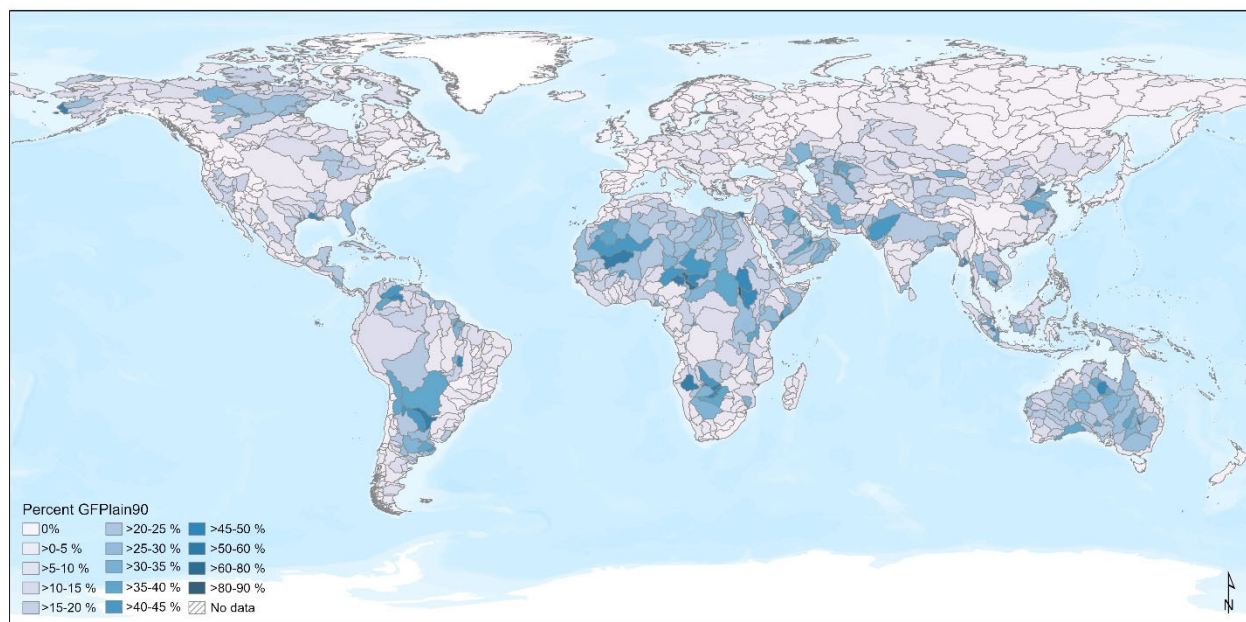
519 **3.3.1 Floodplains**

520

521 Floodplains were estimated to cover 26.6 million km² (Table 5), or 19.7 % of the global landmass.

522 Approximately 23-24 % of the African and Australasian land masses were categorized as occurring

523 within a floodplain, the greatest percentage of global areas so categorized. Conversely, the Arctic
524 (northern Canada and Alaska) and Greenland (excluding the ice sheet) had the least land mass categorized
525 as floodplain (13-14 %). In comparison, Nardi et al. (2019) calculated a global floodplain extent of
526 13,394,139 km², using a 250-m pixel size, a 1000 km² minimum contributing area, and bounding their
527 study between 60° N and 60° S latitudes. Our analyses using the same latitudinal bounds but with a higher
528 resolution dataset (90 m) and a 20 km² minimum contributing area identified 24,185,775 km², an 81 %
529 areal increase (Fig. B1). The relative percent composition of each HydroBASIN that is comprised of
530 GFPlain90 floodplains is given in Fig. 5.
531



532
533 **Figure 5.** Floodplain extents derived from GFPlain90 as a proportion of each of the Level 4 HydroBASINS
534 (Lehrner and Grill, 2013). The data range demonstrated that up to ~90 % of a given watershed was comprised of
535 floodplain area, as evidenced by HydroBASINS in south central Africa and central South America. The basemap
536 layer is the ESRI World Terrain Base (2022).

537
538

539 **Table 5.** Calculated floodplain area for each HydroBASINS at the global scale. Our analyses found 19.7 % of the
 540 landmass occurs within a floodplain.

HydroBASINS Region	Floodplain (km²)	Floodplain Percent of Landmass
Africa	6,990,859	23.3 %
Arctic (northern Canada & Alaska)	894,594	14.2 %
Asia	4,283,991	20.6 %
Australasia	2,649,395	23.8 %
Europe and Middle East	3,415,308	19.1 %
Greenland (excl. ice sheet)	270,813	12.6 %
North & Central America (excl. Alaska)	2,713,346	17.0 %
Siberian Russia	2,051,305	15.8 %
South America	3,368,778	18.9 %
Total	26,638,389	19.7 %

541

542 3.3.2 Wetlands

543

544 Global Wetland extent covered 30.5 million km² (Table 6). With a focus on smaller systems compared to
 545 those presented by Tootchi et al. (2019), our Global Wetland dataset identified 11% more potential global
 546 wetlands (3 million km² additional wetlands). Australasia had the greatest proportional wetland
 547 abundance (see also Zhu et al., 2022), with wetlands covering 38 % of the landmass (driven, in part, by
 548 island abundance and fringing estuarine wetlands [Fan et al., 2013]). Greenland (3 %) and Africa (12 %)
 549 had the least wetlands identified on the land mass.

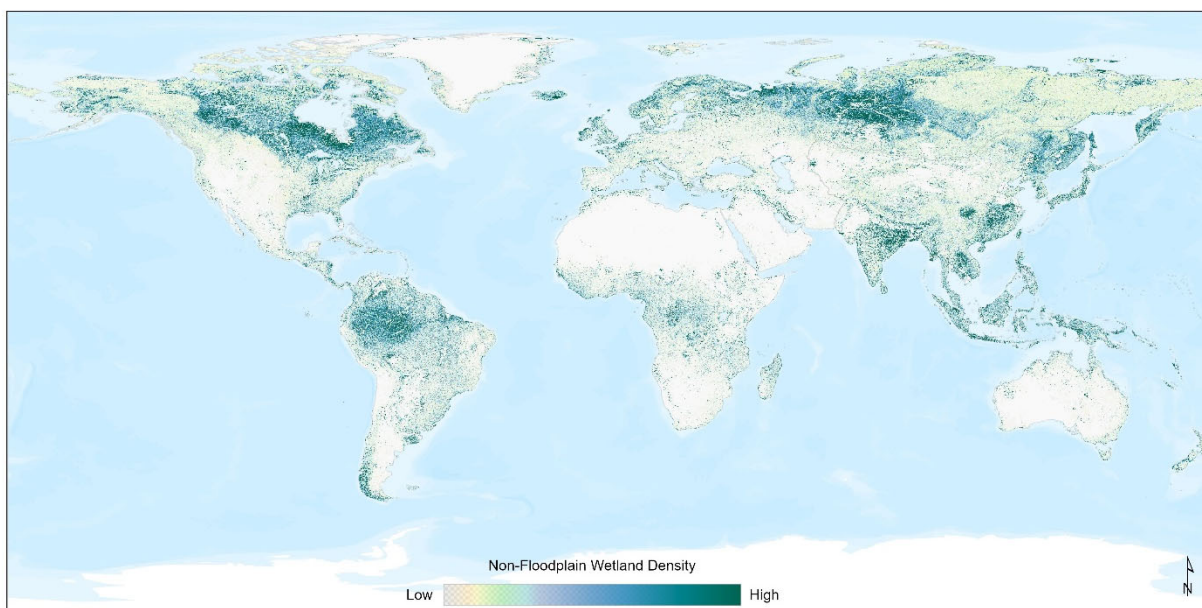
550

551 **Table 6.** Estimated Global Wetlands areal extent for each of the nine regional HydroBASINS (Lehner and Grill,
 552 2013). As described in the text, Global Wetlands extent incorporates the CW-WTD (Tootchi et al., 2019), CCI
 553 (Herold et al., 2015), and GSW (Pekel et al., 2016); lakes of ≥ 10 ha have been removed (Messenger et al., 2016).

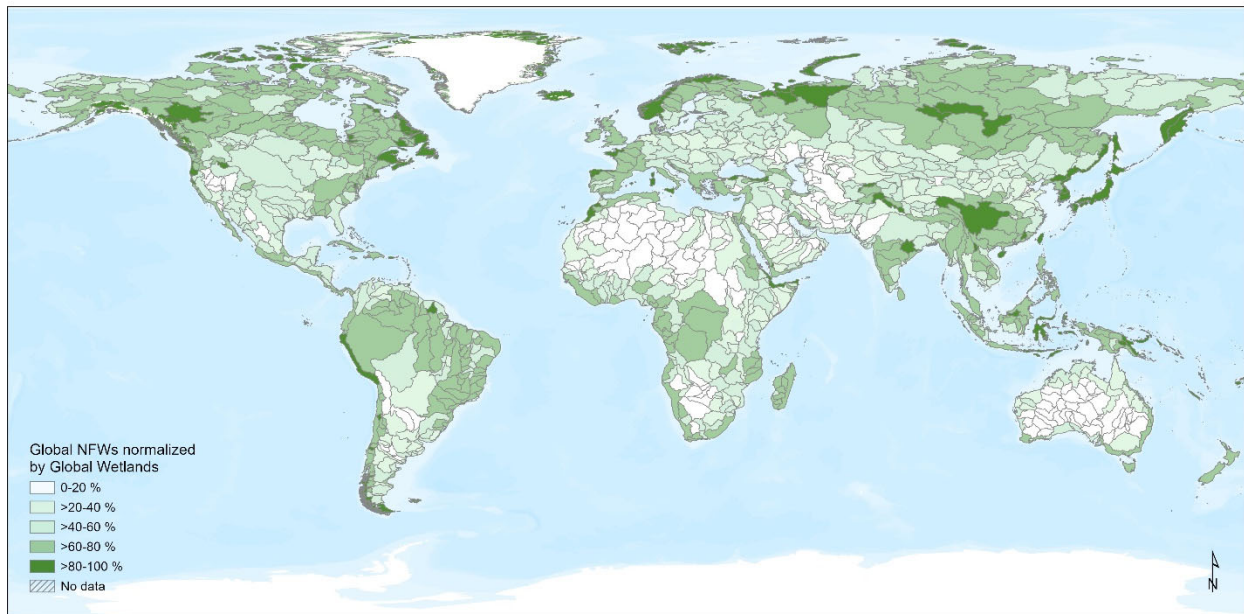
HydroBASINS Region	Wetlands (km²)	Wetland Percent of Landmass
Africa	3,524,917	11.8 %
Arctic (northern Canada & Alaska)	1,807,830	28.6 %
Asia	5,543,333	26.6 %
Australasia	4,283,996	38.4 %
Europe and Middle East	2,465,074	13.8 %
Greenland (excl. ice sheet)	60,761	2.8 %
North & Central America (excl. Alaska)	4,107,333	25.8 %
Siberian Russia	3,578,868	27.6 %
South America	5,140,139	28.8 %
Total	30,512,251	22.6 %

554 3.3.3 Non-floodplain wetlands (Global NFW)

555
556 Approximately 16.0 million km² of potential non-floodplain wetlands were identified globally (Global
557 NFWs, Fig. 6), meaning that 11.9 % of the global landmass is estimated to be covered by non-floodplain
558 wetlands (Table 7). This represents ~53 % of the total global wetlands found in the dataset used in this
559 analysis (see Methods: Wetland Data, above). The global distribution of non-floodplain wetlands is
560 widespread, though they were found to comprise a higher proportion of wetlands within more northern
561 HydroBASINS watersheds (i.e., higher abundances in formerly glaciated basins), as demonstrated in Fig.
562 7. The Arctic portion of northern Canada and Alaska (21.7 %), and Siberian Russia (17.4 %), typically
563 underlain by permafrost and frequently inundated or saturated due to poor drainage evolution
564 (Kremenetski et al., 2003; Robarts et al., 2013; Olefeldt et al., 2021), had the greatest percent non-
565



566
567 **Figure 6.** Non-floodplain wetlands, Global NFWs, are found worldwide, with a greater abundance in formerly
568 glaciated landscapes of northern climates (e.g., northern North America and Siberian Russia) as well as within the
569 Amazon basin (South America). This density map was created using the Focal Statistics tool in ArcGIS Pro 2.9.1.
570 The basemap layer is the ESRI World Terrain Base (2022).



572

573 **Figure 7.** The proportion of non-floodplain wetlands, Global NFWs, within a given HydroBASINS watershed
 574 (Lehrner and Grill, 2013), ranging up to 100 %, varied globally. The impacts or effects of non-floodplain wetlands
 575 on biological, biogeochemical, and hydrological functions will vary based on their relative abundance, location
 576 within the watershed, and hydrologic characteristics (Lane et al., 2018). The basemap layer is the ESRI World
 577 Terrain Base (2022).

578

579 floodplain wetlands. Africa (5.4 %) and Greenland (1.0 %, excluding ice sheets) had the least abundance
 580 of non-floodplain wetlands. A four-direction region-group (contagion) analysis conducted to identify
 581 adjacent pixels considered as contiguous units or non-floodplain wetland systems identified 32.8 million
 582 individual non-floodplain wetlands. Non-floodplain wetlands are typically small aquatic systems (see
 583 Table 7): the median size differed across the HydroBASINS regions from 0.018 km² (1.8 ha) to 0.138
 584 km² (13.8 ha) with a global median of 0.039 km² (3.87 ha).

585 **Table 7.** Global NFW data further described by HydroBASINS region.

HydroBASINS Region	Global NFW Extent (km²)	Count of Global NFWs (#)	Global NFW Percent of Landmass	Global NFW Median Area (km²)
Africa	1,611,225	2,698,465	5.4 %	0.138
Arctic (northern Canada & Alaska)	1,371,937	5,956,081	21.7 %	0.018
Asia	2,924,900	4,564,172	14.0 %	0.049
Australasia	850,402	1,448,315	7.6 %	0.054
Europe and Middle East	1,475,355	3,740,961	8.3 %	0.054
Greenland (excl. ice sheet)	21,747	180,726	1.0 %	0.018
North & Central America (excl. Alaska)	2,608,158	5,740,066	16.4 %	0.025
Siberian Russia	2,255,689	4,864,577	17.4 %	0.063
South America	2,891,604	3,572,294	16.2 %	0.096
Total	16,011,018	32,765,657	11.9 %	0.039

586

587 **4 Discussion**

588

589 We report here for the first time the global abundance of non-floodplain wetlands, a functionally
 590 important and imperiled resource (Creed et al., 2017). Our estimate of 16.0 million km² suggests that
 591 approximately 53 % of the Earth’s wetlands are likely non-floodplain wetland systems. These aquatic
 592 systems are small, with a range from 0.018-0.138 km² (1.8-13.8 ha) across the globe and a global median
 593 size of 0.039 km² (3.87 ha, see Table 7).

594

595 The global abundance of non-floodplain wetlands is a reasonable first approximation of the total non-
 596 floodplain wetland extent. For instance, non-floodplain wetland estimates in the CONUS were conducted
 597 by Lane et al. (2022) using high-resolution aerial-sourced spatial data layers developed by the National
 598 Wetlands Inventory (U.S. Fish and Wildlife Service, various dates). Lane et al. (2022) reported
 599 approximately 23% of the area of freshwater wetlands to be non-floodplain wetland systems. Yet the
 600 CONUS has lost nearly half of its wetlands since the European colonization (Dahl, 1990), with smaller
 601 and shallower non-floodplain wetlands likely being disproportionately lost (Van Meter and Basu, 2015;
 602 Serran et al., 2017).

603

604 Tootchi et al. (2019) – our base input geospatial data layer – calculated that the global wetland extent
605 identified from incorporating both regularly flooded wetland systems (surface-water and precipitation-
606 sourced) and groundwater-driven wetland systems (e.g., Fan et al., 2013; Hu et al., 2017b) resulted in
607 approximately 27.5 million km² of wetlands, a value towards the higher-end of previously published
608 geospatial wetland datasets (Hu et al., 2017a). In their synthesis, Tootchi et al. (2019) explained their
609 values as particularly influenced by groundwater-driven wetlands, especially those in the tropics (10° N-
610 10° S latitudes, Zhu et al., 2022), following recent studies acknowledging the under-estimation of those
611 wetland systems (e.g. Wania et al., 2013; Gumbrecht et al., 2017).

612
613 It follows that incorporating additional higher-resolution satellite inundation data (Pekel et al., 2016) as
614 well as groundwater-driven wetland systems data (e.g., Fan et al., 2013; Tootchi et al., 2019), as
615 conducted in this study, would similarly maintain the trend towards the higher end in global estimates as
616 found by Hu et al. (2017a) and Tootchi et al. (2019). This is meted out in the simple contrast between the
617 proportional abundance of non-floodplain wetland systems identified here against the 30 m NLCD data
618 product described above (Dewitz, 2019) across the 21 CONUS watersheds in this study. The calculated
619 median watershed abundance of non-floodplain wetlands in both the Global NFWs (9.4 %) and the
620 Tootchi et al. (2019) CW-WTD (9.1 %) datasets from our validation watersheds are nearly 5-fold the
621 abundance of the benchmark data from the NLCD (Table 8). However, this is contrasted with a 7-fold
622 *under-representation* of non-floodplain wetlands as derived from the satellite based GSW data (Table 8,
623 Pekel et al., 2016). This suggests that our first approximation of global non-floodplain wetland estimates
624 may be high, primarily due to the resolution of the input data layers. However, as we discuss below,
625 additional factors than just resolution are likely at play.

626
627 It is apparent that the GSW alone is insufficient to map non-floodplain wetlands (this study, Vanderhoof
628 and Lane, 2019). Though useful as a satellite-based input data layer, the GSW by itself appears
629 inadequate for identifying non-floodplain wetlands because it relies on surface-water inundation and

630 ignores saturated wetland systems and those driven by groundwater discharge and upwelling (Winter et
631 al., 1998). Fan et al. (2013) found that groundwater drivers of aquatic system state were important and
632 underrepresented in global datasets. Relying on surface water inundation captured during satellite
633 overflights depends not only on an unobstructed view of the waterbody (e.g., not obscured by trees) but
634 also fortuitous timing regarding inundation status. For example, in an analysis of non-floodplain wetlands
635 of the CONUS as derived by distance from an aquatic system, Lane and D'Amico (2016) reported that
636 just over 50 % of the non-floodplain wetlands were classified as seasonally or temporarily flooded –
637 meaning that cloud-free and unobscured overflights would only potentially identify these systems at
638

639 **Table 8.** A comparison of the non-floodplain wetland distribution within the 21 HUCs contrasting across NLCD
640 (the benchmark data layer, Dewitz, 2019), Global NFW (this study), CW-WTD (Tootchi et al., 2019), and GSW
641 (Pekel et al., 2016). The CW-WTD (at 500 m) and the Global NFW (coupling 500 m, 300 m, and 30 m data),
642 derived from the CW-WTD, identified 5-fold the abundance of non-floodplain wetlands whereas the GSW under-
643 estimated non-floodplain wetlands nearly 7-fold.

HUC ID	Percent HUC as			
	NLCD NFW	Global NFW	CW-WTD NFW	GSW NFW
HUC_0101	10.4 %	19.2 %	18.9 %	0.1 %
HUC_0103	8.1 %	14.6 %	14.3 %	0.2 %
HUC_0106	8.2 %	8.0 %	7.5 %	0.3 %
HUC_0203	4.9 %	8.4 %	8.3 %	0.4 %
HUC_0208	4.7 %	12.0 %	11.5 %	4.6 %
HUC_0304	12.2 %	21.7 %	20.8 %	12.2 %
HUC_0313	8.3 %	14.4 %	13.5 %	8.2 %
HUC_0501	1.5 %	9.2 %	8.9 %	0.1 %
HUC_0706	0.7 %	9.7 %	9.5 %	0.3 %
HUC_0804	9.7 %	17.1 %	16.2 %	9.7 %
HUC_1003	0.7 %	2.1 %	1.9 %	0.2 %
HUC_1015	1.8 %	2.0 %	1.3 %	0.1 %
HUC_1016	3.6 %	16.6 %	15.5 %	2.6 %
HUC_1024	0.5 %	5.1 %	4.9 %	0.2 %
HUC_1029	0.9 %	8.4 %	7.7 %	0.4 %
HUC_1304	0.0 %	5.5 %	5.5 %	0.0 %
HUC_1601	0.7 %	1.3 %	1.0 %	0.1 %
HUC_1708	2.0 %	11.7 %	11.6 %	0.4 %
HUC_1711	1.8 %	9.4 %	9.1 %	0.2 %
HUC_1805	2.2 %	9.9 %	9.7 %	0.5 %
HUC_1808	0.3 %	1.7 %	1.6 %	0.1 %
Median	2.0 %	9.4 %	9.1 %	0.3 %

644

645 certain inundated times of the year. Additionally, Lane and D'Amico (2016) identified another 6 % of
646 CONUS non-floodplain wetlands as saturated (i.e., wetlands with saturated substrates but with surface
647 water seldom present). These wetlands would not be identified by the GSW (Pekel et al., 2016) resulting
648 in a further under-representation of the global resource. Similarly, Hamunyela et al. (2022), analyzing
649 ~150,000 km² in southeastern Africa, found that the GSW underestimated surface water extent (i.e.,
650 omission errors) by nearly 65%. Vanderhoof and Lane (2019) found approximately 42% omission rates
651 when contrasting the GSW data to surface-water extent in non-floodplain wetlands ranging from 0.2-17.6
652 ha in area in the Midwestern US. While the GSW is an outstanding dataset that is continuing to be
653 managed and updated, the GSW and its derived product have limitations in their stand-alone utility in
654 global non-floodplain wetland analyses.

655
656 While solely using satellite-based surface-water data products omits groundwater-driven and saturated
657 wetlands and likely results in non-floodplain wetland underestimations, our Global Wetland data
658 incorporated the finer-resolution CCI (Herold et al., 2015) and GSW (Pekel et al., 2016) products into the
659 Tootchi et al. (2019) base map, substantially improving wetland identification (see Table 3). These
660 improvements, as indicated by performance indices increasing from 10-50 % in the derived Global NFW
661 data (see Table 4), support the inclusion of these higher-resolution satellite-based data (Herold et al.,
662 2015; Pekel et al., 2016) with groundwater datasets (Fan et al., 2013), especially when focused on smaller
663 and non-floodplain wetland systems. Similarly, at a coarser scale of 1 km, there was a difference in Mean
664 Absolute Error value of 0.09 (see Table 4) between the Global NFWs and the benchmark NLCD. This ~9
665 % difference between the two datasets at a 1 km resolution (the former originating at 500 m and the latter
666 at 30 m) further suggest substantive potential utility in these global non-floodplain wetland data for
667 effective natural resource management and decision-making.

668

669

670 **5 Implications**

671
672 Non-floodplain wetlands remain vulnerable waters (Creed et al., 2017; Gardner, 2023), despite the fact
673 that the hydrological, biogeochemical, and biological functions performed by non-floodplain wetlands are
674 increasingly noted in the literature (e.g., Leibowitz, 2003; Creed et al., 2017; Lane et al., 2018; Lane et
675 al., 2022), incorporated into eco-hydrological models by the scientific community (e.g., Fossey and
676 Rousseau, 2016; Golden et al., 2017; Golden et al., 2021; Leibowitz et al., 2023), and considered by
677 policy makers (e.g., Biggs et al., 2017; Drenkhan et al., 2022). Their global fate has important
678 implications for watershed-scale resilience to changing climatic conditions (Mckenna et al., 2017; Lane et
679 al., 2022) affecting the measured benefits humans receive from biogeochemical processing, stormwater
680 attenuation, and drought mitigation functions provided by non-floodplain wetlands.

681
682 Global attention to functions of non-floodplain wetlands has increased in the United States (Marton et al.,
683 2015; Rains et al., 2016; Cohen et al., 2016), Europe (Biggs et al., 2017; Nitzsche et al., 2017; Rodríguez-
684 Rodríguez et al., 2021), Asia (Kam, 2010; Van Meter et al., 2014), Australia (Adame et al., 2019), Africa
685 (Merken et al., 2015; Samways et al., 2020), South America (Rodrigues et al., 2012; Cunha et al., 2019)
686 and elsewhere (see extensive review in Chen et al., 2022). This includes analyses of non-floodplain
687 wetlands both as individual systems (e.g., assessing the functions of a single wetland or wetland complex;
688 Badiou et al., 2018) as well as agglomerated, watershed-scale functioning systems (e.g., answering
689 questions on the functional contributions of all non-floodplain wetlands at larger spatial extents; Golden
690 et al., 2016; Blanchette et al., 2022). Previous studies found that non-floodplain wetlands are
691 overwhelmingly important contributors to biogeochemical and hydrological functions affecting
692 downgradient (i.e., down-stream) water quality and streamflow (e.g., McLaughlin et al., 2014; Marton et
693 al., 2015; Cohen et al., 2016; Rains et al., 2016; Golden et al., 2019; Cheng et al., 2020). Hence, with the
694 development of this publicly available dataset, and subsequent improvements by others, it is hoped that

695 these important aquatic systems will be incorporated into resource management and decision-making
696 across the globe.

697

698 Recently, Lane et al. (2022) identified global-scale geospatial data of the spatial extent and spatial
699 configuration of vulnerable waters – non-floodplain wetlands and headwater stream systems (e.g.,
700 ephemeral, intermittent, and perennial low-order waters [Strahler, 1957]) – as a critical scientific gap.
701 Discounting their significance in watershed-scale hydrology and nutrient biogeochemistry analyses – as
702 well as their importance in biological processes (Schofield et al., 2018; Smith et al., 2019; Mushet et al.,
703 2019) – affects quantification of the myriad ecosystem services they provide (De Groot, 2006; Colvin et
704 al., 2019). For instance, Golden et al. (2021) provide a tangible example of the functional effects and
705 influence of non-floodplain wetlands once incorporated into watershed-scale hydrologic models (Fig. 8):
706 ignoring non-floodplain wetlands in their model resulted in projected critical flood-stage return intervals
707 (e.g., 50 yr and 100 yr floods) being reached within a given modeled time frame. Conversely,
708 incorporating non-floodplain wetlands and their storage capacities into a river basin model (e.g., Rajib et
709 al., 2020) demonstrated that non-floodplain wetlands significantly attenuate storm flows, for when non-
710 floodplain wetlands are “...integrated into the model, those simulated *flood stages are not reached*”
711 (Golden et al., 2021, p. 3, emphasis added). The hydrological functions and concomitantly the associated
712 biogeochemical functions (e.g., Marton et al., 2015) of non-floodplain wetlands demand an effective
713 accounting of their spatial extent and configuration, as demonstrated in this novel global dataset.

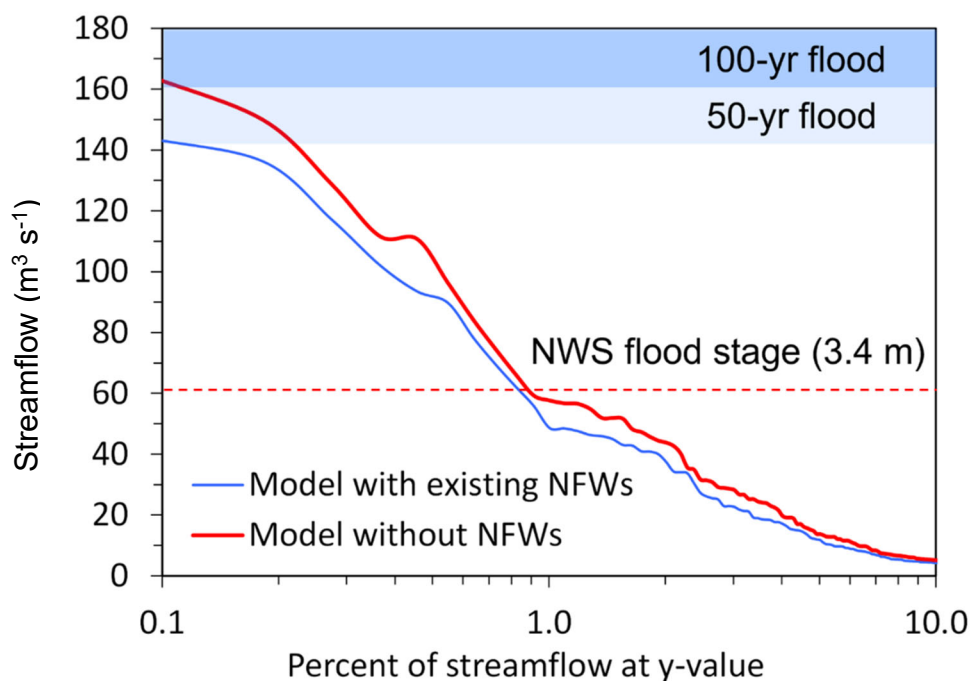
714

715 **6 Global Non-Floodplain Wetlands: Continuing advancements and conclusion**

716

717 Noting the challenges in accurately identifying non-floodplain wetlands – including small size, frequent
718 non-perennial hydrological inundation, soil saturation rather than overlying surface water, and canopy or
719 cloud cover obstructing satellite or airborne detection – recommendations for advanced analyses of non-
720 floodplain wetland extent hinge initially on the use of ancillary data sources. For instance, global

721 assessments will be improved through wall-to-wall high resolution digital elevation models that are used
 722 to identify depressions on the landscape (e.g., Wu et al., 2019b). Though not all landscape depressions are
 723 non-floodplain wetlands (or wetlands at all), analyses that include depressions may find improved
 724 performance when used in combination with vegetation-based assessments or spectral analyses
 725 identifying water (Devries et al., 2017; Evenson et al., 2018b). Similarly, emerging synthetic aperture
 726 radar-based landscape classifications (e.g., Huang et al., 2018; Martinis et al., 2022; Brown et al., 2022)
 727 and both airborne and satellite-borne hyperspectral and advanced analyses, including LiDAR, as well as
 728
 729



730
 731 **Figure 8.** Non-floodplain wetlands attenuate storm flows and decrease flooding hazards. In this example from
 732 Golden et al. (2021, used by permission under Creative Commons Attribution 4.0 license), incorporating the
 733 floodwater storage and attenuation functions of non-floodplain wetlands (NFWs, here) resulted in substantive
 734 decreases in flood-stage heights (i.e., modeled stream outcomes incorporating non-floodplain wetlands reached
 735 neither 50 yr nor 100 yr floods extents). The data from Golden et al. (2021) is of USGS Pipestem Creek gage
 736 06469400, draining approximately 1,800 km².

737 Analytical capabilities (e.g., machine-learning approaches, object-oriented classifications, Berhane et al.,
738 2018); topographically based models, Xi et al., 2022; see Table B1) hold great promise for improved
739 resolution and performance in identifying non-floodplain wetlands (Christensen et al., 2022).

740
741 The Global NFW dataset is not perfect, yet it incrementally advances the current understanding of the
742 potential extent of this important aquatic resource. Limitations of the global dataset (see also Section 4)
743 include the error-propagation and imperfections of the input data layers, including the relatively coarse
744 nature of four of the main input data layers (i.e., the 1000 m groundwater data from Fan et al. (2013), 500
745 m CW-WTD from Tootchi et al. (2019), 500 m GIEMS-D15 from Fluet-Chouinard et al. (2015), and the
746 300 m CCI from Herold et al. (2015)) relative to the target wetland size, as clearly evident in Fig. 4. We
747 additionally acknowledge that omission and commission errors remain within this global data product.
748 For instance, our floodplain-masking process may have inadvertently misassigned pixels derived at 500 m
749 into either non-floodplain or floodplain groups. Though data were not lost when we resampled
750 downwards to 30 m from 500 m, the topological relationships were not necessarily maintained, adding
751 error to the determination of floodplain or non-floodplain pixel status (especially as it relates to those
752 pixels proximate to floodplains). Though imperfect, we suggest Global NFW data should be cautiously
753 incorporated into hydrological, biogeochemical, and biological models to account for the important
754 functions non-floodplain wetlands perform.

755
756 Similarly, though this Global NFW is a static data layer, land use, development, and climate changes
757 continue to affect the prevalence of wetlands worldwide. Fluet-Chouinard et al. (2023) recently noted a
758 global wetland loss of 21% since 1700, with rapid increases from 1950s onwards. Returning to the
759 identification of wetlands and their spatial location vis-à-vis floodplains, using the preponderance of
760 higher-resolution (i.e., < 30 m) and high-return interval sensors will improve both the spatial and
761 temporal accuracy of these data, decreasing commission and omission errors (e.g., Table 8) while

762 increasing the accurate identification of smaller aquatic features that occasional cease to hold standing
763 water.

764

765 The keys to quantifying the functional contributions, ecosystem services, and watershed-scale resilience
766 conferred by non-floodplain wetlands through hydrological, biogeochemical, and biological processes are
767 found through, as a first principle, identifying the spatial extent and configuration of this disappearing and
768 imperiled aquatic system (Creed et al., 2017; Lane et al., 2022). This novel geospatial dataset, freely
769 available (https://gaftp.epa.gov/EPADDataCommons/ORD/Global_NonFloodplain_Wetlands/, Lane et al.,
770 2023), provides for sustainable management of an important aquatic resource and advances the global
771 assessment of non-floodplain wetland functions by facilitating non-floodplain wetland inclusion in both
772 existing models and those under development (Golden et al., 2021).

773

774 **7 Data availability**

775

776 The data are available on the United State Environmental Protection Agency’s Environmental Dataset
777 Gateway (DOI: <https://doi.org/10.23719/1528331>, Lane et al., 2023) or
778 https://gaftp.epa.gov/EPADDataCommons/ORD/Global_NonFloodplain_Wetlands/, (last accessed
779 12/06/2022). Here, we provide global gridded floodplain (90 m, GFPLain90, ~/Global_Floodplains),
780 global gridded wetlands (30 m, Global Wetlands, ~/Global_Wetlands), and global gridded non-floodplain
781 wetlands (30 m, Global NFWs, ~/Global_NFWs) for each of the 1342 HydroBASINS, organized by
782 HydroBASINS region (see, e.g., Table 7).

783

784 **Author contributions.** CL, JC, HG, and ED conceptualized the study, developed the formal analysis, and
785 conducted and/or assisted the data validation. CL wrote and edited the manuscript, while JC and HG
786 reviewed and edited the manuscript. ED also developed the methodology, curated the data, conducted the
787 formal spatial analysis, validated the data, visualized the data, and reviewed and edited the manuscript.

788 QW and AR assisted in methodology development, validated the study outputs, conducted formal
789 analyses, and reviewed and edited the manuscript.

790

791 **Competing interests.** The corresponding authors have declared that none of the authors have any
792 competing interests.

793

794 **Disclaimer.** Publisher’s note: Copernicus Publications remains neutral with regard to jurisdictional
795 claims in published maps and institutional affiliations.

796

797 **Acknowledgements.** We greatly appreciate the scientific contributions and stimulative discussions in the
798 papers led by Ardalan Tootchi, Sean Woznicki, Fernando Nardi, Oliver Wing, Paul Bates, and their co-
799 authors that inspired us to complete these analyses. Jeremy Baynes and John Johnston conducted critical
800 reviews to improve this manuscript, and their efforts are acknowledged. This paper has been reviewed in
801 accordance with the US Environmental Protection Agency’s peer and administrative review policies and
802 approved for publication. Mention of trade names or commercial products does not constitute
803 endorsement or recommendation for use. Statements in this publication reflect the authors’ professional
804 views and opinions and should not be construed to represent any determination or policy of the US
805 Environmental Protection Agency.

806

807 **Review statement.** This paper was edited by Yuanzhi Yao and reviewed by Youjiang Shen and Michele
808 Ronco.

809

810 **Appendix A: Abbreviations**

811	AEB	Aggregate error bias
812	CaMa-Flood	Catchment-based Macro-scale Floodplain
813	CCI	Climate change initiative

814	CIMA-UNEP	CIMA Research Foundation - United Nations Environmental Programme
815	CONUS	Conterminous United States
816	CSI	Critical Success Index
817	CW-WTD	Composite wetland-water table depth
818	DEM	Digital elevation model
819	EB	Error Bias
820	ECMWF	European Centre for Medium-Range Weather Forecasts
821	EPA	Environmental Protection Agency
822	ESA	European Space Agency
823	FA	False Alarm
824	FEMA	Federal Emergency Management Agency
825	GDW	Groundwater-driven wetlands
826	GFPlain	Global Floodplain
827	GIEMS-D15	Global Inundation Extent from Multi-Satellites Downscaled - 15 arcseconds
828	GIS	Geographic information systems
829	GLOFRIS	Global Flood Risk with Image Scenarios
830	GLWD	Global Lakes and Wetlands Database
831	GNFW	Global Non-floodplain wetlands
832	GSW	Global surface water
833	GW	Global wetlands
834	H	Hit Rate
835	HUC	Hydrologic unit code
836	IPCC	Intergovernmental Panel on Climate Change
837	JRC	Joint Research Center
838	LIDAR	Light detection and ranging
839	MAE	Mean absolute error

840	MERIT	Multi-Error Removed Improved Terrain
841	ML	Machine learning
842	NFW	Non-floodplain wetland
843	NLCD	National Land Cover Database
844	NWS	National Weather Service
845	P	Precision
846	RFW	Regularly flooded wetland
847	SAR	Synthetic aperture radar
848	USA	United States of America
849	USGS	United States Geological Survey
850	UTM	Universal Transverse Mercator
851	WTD	Water table depth
852		

853 **Appendix B: Supplemental Tables and Figures**854 **Table B1.** Emerging global land cover datasets related to surface water and wetlands.

Data Set	Resolution	Years of Data	Wetland Classes	Image Sources	Reference and website
ESA WorldCover	10 m	2020-2021	Permanent water bodies; herbaceous wetland; mangroves	Sentinel-1 & Sentinel-2	Zanaga et al. (2021); https://esa-worldcover.org
Esri Global Land Cover	10 m	2017-2022	Water; flooded vegetation	Sentinel-2	Karra et al. (2021); https://livingatlas.arcgis.com/landcover
Dynamic World	10 m	2015-2023	Water; flooded vegetation	Sentinel-2	Brown et al. (2022); https://dynamicworld.app/

855

856

857 **Table B2.** Descriptive characteristics of the 21 verification basins located throughout the CONUS (see Fig. 2).
858 Majority Köppen-Geiger classification follows Beck et al. (2018). Climatological data were acquired from the
859 PRISM Climate Group (Parameter-elevation Regressions on Independent Slopes Model, prism.oregonstate.edu/,
860 accessed 09/26/2022) using the 30-year annual normals for each watershed. Land use data and descriptions are from
861 the 2019 NLCD (www.mrlc.gov/data, accessed 09/26/2022) and represent the land use class with the greatest areal
862 abundance. Average elevation was derived from the USGS National Elevation Dataset (https://www.usgs.gov/3d-
863 elevation-program, accessed 01/13/2022). Global Wetland Count are the counts of wetlands from the derived Global
864 Wetland database within each watershed after region-grouping the data using a four-direction contagion criterion
865 (i.e., pixels immediately adjacent in any of the four cardinal directions are considered part of a unique, multi-pixel
866 wetland, ArcGIS Pro v.2.9.1, Redlands, California).

Hydrologic Unit Code	Area	Köppen-	Mean Annual	Mean Annual
ID	(km ²)	Geiger	Temp (°C)	Rainfall (m)
HUC_0101	18,906	Dfb	4.0	1.1
HUC_0103	15,287	Dfb	5.4	1.2
HUC_0106	10,800	Dfb	7.5	1.3
HUC_0203	12,490	Dfa	11.6	1.2
HUC_0208	47,449	Cfa	13.7	1.2
HUC_0304	47,899	Cfa	16.4	1.3
HUC_0313	52,169	Cfa	18.1	1.4
HUC_0501	30,371	Dfb	8.6	1.2
HUC_0706	22,257	Dfa	8.1	1.0
HUC_0804	53,108	Cfa	17.5	1.4
HUC_1003	51,431	BSk	5.6	0.4
HUC_1015	37,098	Dfa	8.7	0.5
HUC_1016	54,743	Dfa	6.4	0.6
HUC_1024	35,237	Dfa	10.8	0.9
HUC_1029	48,204	Dfa	13.2	1.1
HUC_1304	48,126	BSh	18.6	0.4
HUC_1601	19,463	BSk	5.7	0.5
HUC_1708	16,101	Csb	9.0	2.1
HUC_1711	35,651	Csb	8.2	2.0
HUC_1805	11,341	Csb	14.9	0.7
HUC_1808	11,789	BSk	8.4	0.4

867 † Köppen-Geiger Class Descriptions (Beck et al. 2018): BSh (arid, steppe, hot), BSk (arid, steppe, cold), Cfa
868 (temperate, no dry season, hot summer), Csb, (temperature, dry season, warm summer), Dfa (cold, no dry season,
869 hot summer), Dfb (cold, no dry season, warm summer)

870

871 **Table B2.** (Continued)

Hydrologic Unit	Majority Land	Majority Land	Global Wetland	Average
Code	Use Coverage	Coverage Description	Count	Elevation
HUC_0101	43	Mixed Forest	2,141	296
HUC_0103	43	Mixed Forest	2,202	300
HUC_0106	43	Mixed Forest	2,799	169
HUC_0203	41	Deciduous Forest	2,438	82
HUC_0208	41	Deciduous Forest	13,934	187
HUC_0304	90	Woody Wetlands	14,643	127
HUC_0313	42	Evergreen Forest	27,056	147
HUC_0501	41	Deciduous Forest	6,310	484
HUC_0706	82	Cultivated Crops	3,100	300
HUC_0804	42	Evergreen Forest	12,242	85
HUC_1003	71	Herbaceous	11,852	1349
HUC_1015	71	Herbaceous	8,628	961
HUC_1016	82	Cultivated Crops	61,482	464
HUC_1024	82	Cultivated Crops	11,995	341
HUC_1029	81	Hay/Pasture	23,935	297
HUC_1304	52	Shrub/Scrub	1,733	995
HUC_1601	52	Shrub/Scrub	2,642	1981
HUC_1708	42	Evergreen Forest	1,986	552
HUC_1711	42	Evergreen Forest	6,562	621
HUC_1805	52	Shrub/Scrub	1,208	222
HUC_1808	52	Shrub/Scrub	1,089	1625

872

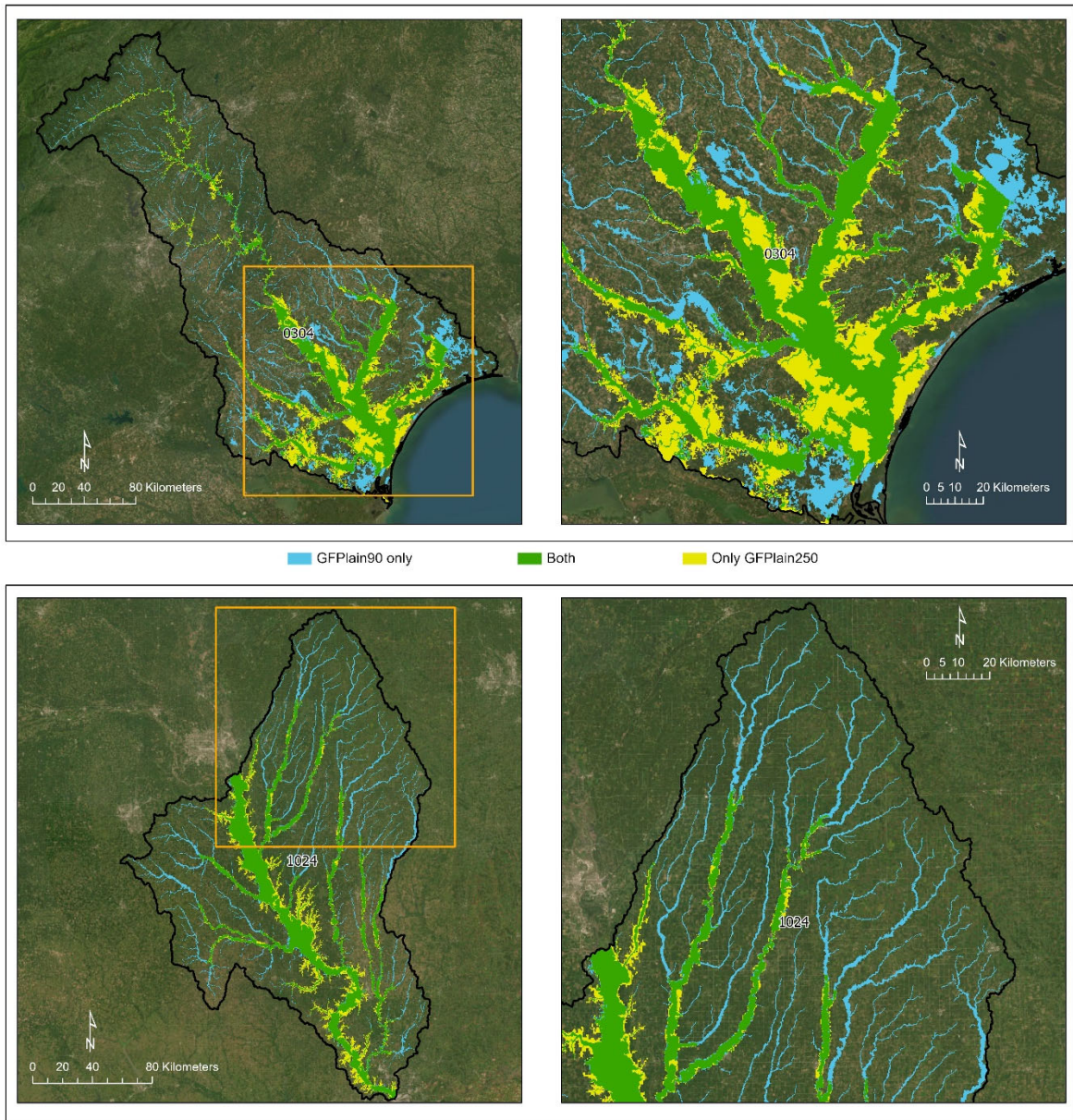
873

874 **Table B3.** Floodplain performance assessment of the GFPlain90-derived floodplain and the benchmark floodplain
875 from Woznicki et al. (2019). The first six equations directly assess the spatial concordance and overlap between the
876 two datasets, whereas Mean Absolute Error (Eq. 7) and Aggregate Error Bias (Eq. 8) are coarser fractional analyses
877 (i.e., the fraction of a 1 km² cell predicted correctly) as measured along the riverine network.

Hydrologic Unit Code (HUC) ID	Hit Rate	Precision	False Alarm	CSI	F1	Error Bias	Mean Absolute Error	Aggregate Error Bias
	(Eq. 1)	(Eq. 2)	(Eq. 3)	(Eq. 4)	(Eq. 5)	(Eq. 6)	(Eq. 7)	(Eq. 8)
HUC_0101	0.76	0.84	0.16	0.66	0.80	0.62	0.06	-0.01
HUC_0103	0.92	0.77	0.23	0.72	0.84	3.25	0.05	0.03
HUC_0106	0.78	0.74	0.26	0.62	0.76	1.24	0.10	-0.03
HUC_0203	0.47	0.58	0.42	0.35	0.52	0.66	0.25	-0.18
HUC_0208	0.64	0.73	0.27	0.52	0.68	0.67	0.13	-0.08
HUC_0304	0.63	0.81	0.19	0.55	0.71	0.41	0.06	0.00
HUC_0313	0.62	0.72	0.28	0.50	0.67	0.62	0.09	-0.01
HUC_0501	0.77	0.85	0.15	0.68	0.81	0.59	0.04	-0.02
HUC_0706	0.86	0.79	0.21	0.69	0.82	1.62	0.04	0.02
HUC_0804	0.75	0.83	0.17	0.65	0.79	0.64	0.08	-0.02
HUC_1003	0.85	0.42	0.58	0.39	0.56	7.70	0.11	0.09
HUC_1015	0.81	0.74	0.26	0.63	0.78	1.54	0.06	0.02
HUC_1016	0.89	0.36	0.64	0.35	0.52	14.79	0.18	0.17
HUC_1024	0.90	0.88	0.12	0.80	0.89	1.19	0.03	0.00
HUC_1029	0.84	0.87	0.13	0.75	0.85	0.82	0.04	-0.01
HUC_1304	0.66	0.74	0.26	0.53	0.70	0.67	0.07	-0.01
HUC_1601	0.92	0.55	0.45	0.52	0.69	9.47	0.10	0.08
HUC_1708	0.60	0.71	0.29	0.48	0.65	0.60	0.08	-0.03
HUC_1711	0.70	0.50	0.50	0.41	0.58	2.25	0.10	-0.02
HUC_1805	0.59	0.59	0.41	0.41	0.59	1.00	0.14	-0.05
HUC_1808	0.98	0.44	0.56	0.44	0.61	82.97	0.24	0.23
Median	0.77	0.74	0.26	0.53	0.70	1.00	0.08	-0.01
Mean	0.76	0.69	0.31	0.56	0.71	6.35	0.10	0.01

878

879



880
 881 **Figure B1.** Comparison of floodplain extents derived from GFPlain90 (this study) and GFPlain250 (Nardi et al.,
 882 2019). The right-hand panels are the inset area outlined in the orange box on the left panels; the top panels represent
 883 an eastern coastal watershed (HUC_0304) whereas the bottom panels are from a Midwestern US watershed
 884 (HUC_1024). The full extent of the riverine network is evident in the GFPlain90 dataset, which was derived from 90
 885 m resolution DEMs in contrast to the 250 m pixel size of the GFPlain250. Satellite imagery sourced from ESRI
 886 (2022).

887 **References**

888

889 Adame, M. F., Arthington, A. H., Waltham, N., Hasan, S., Selles, A., and Ronan, M.: Managing threats
890 and restoring wetlands within catchments of the Great Barrier Reef, Australia, *Aquatic Conservation:
891 Marine and Freshwater Ecosystems*, 29, 829-839, <https://doi.org/10.1002/aqc.3096>, 2019.

892 Alfieri, L., Salamon, P., Bianchi, A., Neal, J., Bates, P., and Feyen, L.: Advances in pan-European flood
893 hazard mapping, *Hydrological Processes*, 28, 4067-4077, 10.1002/hyp.9947, 2014.

894 Ameli, A. A. and Creed, I. F.: Does Wetland Location Matter When Managing Wetlands for Watershed-
895 Scale Flood and Drought Resilience?, *JAWRA Journal of the American Water Resources Association*,
896 55, 529-542, 10.1111/1752-1688.12737, 2019.

897 Aronica, G., Bates, P. D., and Horritt, M. S.: Assessing the uncertainty in distributed model predictions
898 using observed binary pattern information within GLUE, *Hydrological Processes*, 16, 2001-2016,
899 <https://doi.org/10.1002/hyp.398>, 2002.

900 Assessment, M. E.: *Ecosystems and Human Well-Being: Wetlands and Water Synthesis*, World
901 Resources Institute, Washington, D.C., 2005.

902 Badiou, P., Page, B., and Akinremi, W.: Phosphorus Retention in Intact and Drained Prairie Wetland
903 Basins: Implications for Nutrient Export, *Journal of Environmental Quality*, 47, 902-913,
904 <https://doi.org/10.2134/jeq2017.08.0336>, 2018.

905 Bam, E. K. P., Ireson, A. M., van der Kamp, G., and Hendry, J. M.: Ephemeral Ponds: Are They the
906 Dominant Source of Depression-Focused Groundwater Recharge?, *Water Resources Research*, 56,
907 e2019WR026640, <https://doi.org/10.1029/2019WR026640>, 2020.

908 Bates, P. D. and De Roo, A. P. J.: A simple raster-based model for flood inundation simulation, *Journal of*
909 *Hydrology*, 236, 54-77, [http://dx.doi.org/10.1016/S0022-1694\(00\)00278-X](http://dx.doi.org/10.1016/S0022-1694(00)00278-X), 2000.

910 Beck, H. E., Zimmermann, N. E., McVicar, T. R., Vergopolan, N., Berg, A., and Wood, E. F.: Present
911 and future Köppen-Geiger climate classification maps at 1-km resolution, *Scientific Data*, 5, 180214,
912 10.1038/sdata.2018.214, 2018.

913 Berhane, T., Lane, C., Wu, Q., Autrey, B., Anenkhonov, O., Chepinoga, V., and Liu, H.: Decision-Tree,
914 Rule-Based, and Random Forest Classification of High-Resolution Multispectral Imagery for Wetland
915 Mapping and Inventory, *Remote Sensing*, 10, 580, 2018.

916 Biggs, J., von Fumetti, S., and Kelly-Quinn, M.: The importance of small waterbodies for biodiversity
917 and ecosystem services: implications for policy makers, *Hydrobiologia*, 793, 3-39, 10.1007/s10750-
918 016-3007-0, 2017.

919 Blanchette, M., Rousseau, A. N., Savary, S., and Foulon, É.: Are spatial distribution and aggregation of
920 wetlands reliable indicators of stream flow mitigation?, *Journal of Hydrology*, 608, 127646,
921 <https://doi.org/10.1016/j.jhydrol.2022.127646>, 2022.

922 Brown, C. F., Brumby, S. P., Guzder-Williams, B., Birch, T., Hyde, S. B., Mazzariello, J., Czerwinski,
923 W., Pasquarella, V. J., Haertel, R., Ilyushchenko, S., Schwehr, K., Weisse, M., Stolle, F., Hanson, C.,
924 Guinan, O., Moore, R., and Tait, A. M.: Dynamic World, Near real-time global 10 m land use land
925 cover mapping, *Scientific Data*, 9, 251, 10.1038/s41597-022-01307-4, 2022.

926 Buttle, J. M.: Mediating stream baseflow response to climate change: The role of basin storage,
927 *Hydrological Processes*, 32, 363-378, 10.1002/hyp.11418, 2018.

928 Chen, J., Chen, J., Liao, A., Cao, X., Chen, L., Chen, X., He, C., Han, G., Peng, S., Lu, M., Zhang, W.,
929 Tong, X., and Mills, J.: Global land cover mapping at 30m resolution: A POK-based operational
930 approach, *ISPRS Journal of Photogrammetry and Remote Sensing*, 103, 7-27,
931 <https://doi.org/10.1016/j.isprsjprs.2014.09.002>, 2015.

932 Chen, W., Thorslund, J., Nover, D. M., Rains, M. C., Li, X., Xu, B., He, B., Su, H., Yen, H., Liu, L.,
933 Yuan, H., Jarsjö, J., and Viers, J. H.: A typological framework of non-floodplain wetlands for global
934 collaborative research and sustainable use, *Environmental Research Letters*, 17, 113002, 10.1088/1748-
935 9326/ac9850, 2022.

936 Cheng, F. Y. and Basu, N. B.: Biogeochemical hotspots: Role of small water bodies in landscape nutrient
937 processing, *Water Resources Research*, 53, 5038-5056, 10.1002/2016WR020102, 2017.

938 Cheng, F. Y., Van Meter, K. J., Byrnes, D. K., and Basu, N. B.: Maximizing US nitrate removal through
939 wetland protection and restoration, *Nature*, 588, 625-630, 10.1038/s41586-020-03042-5, 2020.

940 Christensen, J. R., Golden, H. E., Alexander, L. C., Pickard, B. R., Fritz, K. M., Lane, C. R., Weber, M.
941 H., Kwok, R. M., and Keefer, M. N.: Headwater streams and inland wetlands: Status and advancements
942 of geospatial datasets and maps across the United States, *Earth-Science Reviews*, 104230,
943 <https://doi.org/10.1016/j.earscirev.2022.104230>, 2022.

944 Cohen, M. J., Creed, I. F., Alexander, L., Basu, N. B., Calhoun, A. J. K., Craft, C., D'Amico, E.,
945 DeKeyser, E., Fowler, L., Golden, H. E., Jawitz, J. W., Kalla, P., Kirkman, L. K., Lane, C. R., Lang,
946 M., Leibowitz, S. G., Lewis, D. B., Marton, J., McLaughlin, D. L., Mushet, D. M., Raanan-Kiperwas,
947 H., Rains, M. C., Smith, L., and Walls, S. C.: Do geographically isolated wetlands influence landscape
948 functions?, *Proceedings of the National Academy of Sciences*, 113, 1978-1986,
949 10.1073/pnas.1512650113, 2016.

950 Colvin, S. A. R., Sullivan, S. M. P., Shirey, P. D., Colvin, R. W., Winemiller, K. O., Hughes, R. M.,
951 Fausch, K. D., Infante, D. M., Olden, J. D., Bestgen, K. R., Danchy, R. J., and Eby, L.: Headwater
952 Streams and Wetlands are Critical for Sustaining Fish, Fisheries, and Ecosystem Services, *Fisheries*, 44,
953 73-91, 2019.

954 Cowardin, L. M., Carter, V., Golet, F. C., and LaRoe, E. T.: Classification of Wetlands and Deepwater
955 habitats of The United States, Fish and Wildlife Service, Washington DCFWS/OBS-79/31, 1979.

956 Creed, I. F., Lane, C. R., Serran, J. N., Alexander, L. C., Basu, N. B., Calhoun, A. J. K., Christensen, J.
957 R., Cohen, M. J., Craft, C., D'Amico, E., DeKeyser, E., Fowler, L., Golden, H. E., Jawitz, J. W., Kalla,
958 P., Kirkman, L. K., Lang, M., Leibowitz, S. G., Lewis, D. B., Marton, J., McLaughlin, D. L., Raanan-
959 Kiperwas, H., Rains, M. C., Rains, K. C., and Smith, L.: Enhancing protection for vulnerable waters,
960 *Nature Geoscience*, 10, 809-815, 10.1038/ngeo3041, 2017.

961 Cunha, D. G. F., Magri, R. A. F., Tromboni, F., Ranieri, V. E. L., Fendrich, A. N., Campanhão, L. M. B.,
962 Riveros, E. V., and Velázquez, J. A.: Landscape patterns influence nutrient concentrations in aquatic

963 systems: citizen science data from Brazil and Mexico, *Freshwater Science*, 38, 365-378,
964 10.1086/703396, 2019.

965 Dahl, T. E.: *Wetlands - Losses in the United States, 1780's to 1980's*, U.S. Department of Interior, Fish
966 and Wildlife Service Washington DC, 1990.

967 Davidson, N. C.: How much wetland has the world lost? Long-term and recent trends in global wetland
968 area, *Marine and Freshwater Research*, 65, 934-941, <http://dx.doi.org/10.1071/MF14173>, 2014.

969 Davidson, N. C., E. Fluet-Chouinard and C. M. Finlayson. 2018. Global extent and distribution of
970 wetlands: trends and issues. *Marine and Freshwater Research* 69, 4, 620-627, 2018.

971 De Groot, R., M. Stuij, M. Finlayson, and N. Davidson: *Valuing Wetlands: Guidance for Valuing the*
972 *Benefits Derived from Wetland Ecosystem Services*, Ramsar Convention Secretariat, Gland,
973 Switzerland and Secretariat of the Convention on Biological Diversity, Montreal, Canada, Gland,
974 Switzerland Ramsar Technical Report No. 3/CBD Technical Series No. 27, 2006.

975 DeVries, B., Huang, C., Lang, M., Jones, J., Huang, W., Creed, I., and Carroll, M.: Automated
976 Quantification of Surface Water Inundation in Wetlands Using Optical Satellite Imagery, *Remote*
977 *Sensing*, 9, 807, 2017.

978 Dewitz, J.: National Land Cover Database (NLCD) 2016 Products: U.S. Geological Survey data release
979 [dataset], <https://doi.org/10.5066/P96HHBIE>, 2019.

980 Drenkhan, F., Buytaert, W., Mackay, J. D., Barrand, N. E., Hannah, D. M., and Huggel, C.: Looking
981 beyond glaciers to understand mountain water security, *Nature Sustainability*, 10.1038/s41893-022-
982 00996-4, 2022.

983 ESA Worldwide Land Cover Mapping: <https://esa-worldcover.org/en>, last access: 22 December 2022.
984 ESA Land Cover CCI, Product User Guide Version 2.0:
985 https://maps.elie.ucl.ac.be/CCI/viewer/download/ESACCI-LC-Ph2-PUGv2_2.0.pdf, last access: May
986 2022.

987 ESRI World Terrain Base
988 <https://www.arcgis.com/home/item.html?id=be2e229ffc864c868a78f5ca68ca5b8e>, last accessed 22
989 December 2022.

990 Evenson, G. R., Golden, H. E., Lane, C. R., McLaughlin, D. L., and D'Amico, E.: Depressional Wetlands
991 Affect Watershed Hydrological, Biogeochemical, and Ecological Functions, *Ecological Applications*,
992 28, 953-966, 10.1002/eap.1701, 2018a.

993 Evenson, G. R., Jones, C. N., McLaughlin, D. L., Golden, H. E., Lane, C. R., DeVries, B., Alexander, L.
994 C., Lang, M. W., McCarty, G. W., and Sharifi, A.: A watershed-scale model for depressional wetland-
995 rich landscapes, *Journal of Hydrology X*, 1, 100002, <https://doi.org/10.1016/j.hydroa.2018.10.002>,
996 2018b.

997 Evenson, G. R., Golden, H. E., Christensen, J. R., Lane, C. R., Rajib, A., D'Amico, E., Mahoney, D. T.,
998 White, E., and Wu, Q.: Wetland restoration yields dynamic nitrate responses across the Upper
999 Mississippi river basin, *Environmental Research Communications*, 3, 095002, 10.1088/2515-
1000 7620/ac2125, 2021.

1001 Fan, Y., Li, H., and Miguez-Macho, G.: Global Patterns of Groundwater Table Depth, *Science*, 339, 940-
1002 943, doi:10.1126/science.1229881, 2013.

1003 Fewtrell, T. J., Bates, P. D., Horritt, M., and Hunter, N. M.: Evaluating the effect of scale in flood
1004 inundation modelling in urban environments, *Hydrological Processes*, 22, 5107-5118,
1005 <https://doi.org/10.1002/hyp.7148>, 2008.

1006 Fluet-Chouinard, E., Lehner, B., Rebelo, L.-M., Papa, F., and Hamilton, S. K.: Development of a global
1007 inundation map at high spatial resolution from topographic downscaling of coarse-scale remote sensing
1008 data, *Remote Sensing of Environment*, 158, 348-361, <https://doi.org/10.1016/j.rse.2014.10.015>, 2015.

1009 Fluet-Chouinard, E., B. D. Stocker, Z. Zhang, A. Malhotra, J. R. Melton, B. Poulter, J. O. Kaplan, K. K.
1010 Goldewijk, S. Siebert, T. Minayeva, G. Hugelius, H. Joosten, A. Barthelmes, C. Prigent, F. Aires, A. M.
1011 Hoyt, N. Davidson, C. M. Finlayson, B. Lehner, R. B. Jackson and P. B. McIntyre. Extensive global
1012 wetland loss over the past three centuries, *Nature*, 614, 7947, 281-286, 2023.

1013 Fossey, M. and Rousseau, A. N.: Can isolated and riparian wetlands mitigate the impact of climate
1014 change on watershed hydrology? A case study approach, *Journal of Environmental Management*,
1015 184(2):327-339, <http://dx.doi.org/10.1016/j.jenvman.2016.09.043>, 2016.

1016 Gardner, R.: What the US Supreme Court decision means for wetlands, *Nature*, 618, 215,
1017 doi.org/10.1038/d41586-023-01827-y

1018 Golden, H. E., Lane, C. R., Rajib, A., and Wu, Q.: Improving global flood and drought predictions:
1019 integrating non-floodplain wetlands into watershed hydrologic models, *Environmental Research*
1020 *Letters*, 16, 091002, 10.1088/1748-9326/ac1fbc, 2021.

1021 Golden, H. E., Rajib, A., Lane, C. R., Christensen, J. R., Wu, Q., and Mengistu, S.: Non-floodplain
1022 Wetlands Affect Watershed Nutrient Dynamics: A Critical Review, *Environmental Science &*
1023 *Technology*, 53, 7203-7214, 10.1021/acs.est.8b07270, 2019.

1024 Golden, H. E., Sander, H. A., Lane, C. R., Zhao, C., Price, K., D'Amico, E., and Christensen, J. R.:
1025 Relative effects of geographically isolated wetlands on streamflow: a watershed-scale analysis,
1026 *Ecohydrology*, 9, 21-38, 10.1002/eco.1608, 2016.

1027 Golden, H. E., Creed, I. F., Ali, G., Basu, N. B., Neff, B. P., Rains, M. C., McLaughlin, D. L., Alexander,
1028 L. C., Ameli, A. A., Christensen, J. R., Evenson, G. R., Jones, C. N., Lane, C. R., and Lang, M.:
1029 Integrating geographically isolated wetlands into land management decisions, *Frontiers in Ecology and*
1030 *the Environment*, 15, 319-327, 10.1002/fee.1504, 2017.

1031 Gumbricht, T., Roman-Cuesta, R. M., Verchot, L., Herold, M., Wittmann, F., Householder, E., Herold,
1032 N., and Murdiyarso, D.: An expert system model for mapping tropical wetlands and peatlands reveals
1033 South America as the largest contributor, *Global Change Biology*, 23, 3581-3599,
1034 <https://doi.org/10.1111/gcb.13689>, 2017.

1035 Hamunyela, E., Hipondoka, M., Persendt, F., Sevelia Nghiyalwa, H., Thomas, C., and Matengu, K.:
1036 Spatio-temporal characterization of surface water dynamics with Landsat in endorheic Cuvelai-Etoshia
1037 Basin (1990–2021), *ISPRS Journal of Photogrammetry and Remote Sensing*, 191, 68-84,
1038 <https://doi.org/10.1016/j.isprsjprs.2022.07.007>, 2022.

1039 Hoch, J. M. and M. A. Trigg. Advancing global flood hazard simulations by improving comparability,
1040 benchmarking, and integration of global flood models. *Environmental Research Letters*, 14, 3, 034001,
1041 2019.

1042 Homer, C., Dewitz, J., Jin, S., Xian, G., Costello, C., Danielson, P., Gass, L., Funk, M., Wickham, J.,
1043 Stehman, S., Auch, R., and Riitters, K.: Conterminous United States land cover change patterns 2001–
1044 2016 from the 2016 National Land Cover Database, *ISPRS Journal of Photogrammetry and Remote*
1045 *Sensing*, 162, 184-199, <https://doi.org/10.1016/j.isprsjprs.2020.02.019>, 2020.

1046 Horritt, M. S. and Bates, P. D.: Evaluation of 1D and 2D numerical models for predicting river flood
1047 inundation, *Journal of Hydrology*, 268, 87-99, [http://dx.doi.org/10.1016/S0022-1694\(02\)00121-X](http://dx.doi.org/10.1016/S0022-1694(02)00121-X),
1048 2002.

1049 Hu, S., Niu, Z., and Chen, Y.: Global Wetland Datasets: a Review, *Wetlands*, 37, 807-817,
1050 10.1007/s13157-017-0927-z, 2017a.

1051 Hu, S., Niu, Z., Chen, Y., Li, L., and Zhang, H.: Global wetlands: Potential distribution, wetland loss, and
1052 status, *Science of The Total Environment*, 586, 319-327,
1053 <http://dx.doi.org/10.1016/j.scitotenv.2017.02.001>, 2017b.

1054 Huang, W., DeVries, B., Huang, C., Lang, M., Jones, J., Creed, I., and Carroll, M.: Automated Extraction
1055 of Surface Water Extent from Sentinel-1 Data, *Remote Sensing*, 10, 797, 2018.

1056 IPCC: Intergovernmental Panel on Climate Change 2014: Impacts, adaptation, and vulnerability,
1057 Cambridge University Press, Cambridge, U.K.2014.

1058 Jafarzadegan, K., Merwade, V., and Saksena, S.: A geomorphic approach to 100-year floodplain mapping
1059 for the Conterminous United States, *Journal of Hydrology*, 561, 43-58,
1060 <https://doi.org/10.1016/j.jhydrol.2018.03.061>, 2018.

1061 Jakubínský, J., Prokopová, M., Raška, P., Salvati, L., Bezak, N., Cudlín, O., Cudlín, P., Purkyt, J., Vezza,
1062 P., Camporeale, C., Daněk, J., Pástor, M., and Lepeška, T.: Managing floodplains using nature-based
1063 solutions to support multiple ecosystem functions and services, *WIREs Water*, 8, e1545,
1064 <https://doi.org/10.1002/wat2.1545>, 2021.

1065 Jin, S., Homer, C., Yang, L., Danielson, P., Dewitz, J., Li, C., Zhu, Z., Xian, G., and Howard, D.: Overall
1066 Methodology Design for the United States National Land Cover Database 2016 Products, Remote
1067 Sensing, 11, 2971, 2019.

1068 Jones, C. N., Evenson, G. R., McLaughlin, D. L., Vanderhoof, M. K., Lang, M. W., McCarty, G. W.,
1069 Golden, H. E., Lane, C. R., and Alexander, L. C.: Estimating restorable wetland water storage at
1070 landscape scales, Hydrological Processes, 32, 305-313, 10.1002/hyp.11405, 2018.

1071 Karra, K., Kontgis, C., Statman-Weil, Z., Mazzariello, J. C., Mathis, M., & Brumby, S. P. Global land
1072 use/land cover with Sentinel 2 and deep learning. In: 2021 IEEE International Geoscience and Remote
1073 Sensing Symposium IGARSS (pp. 4704-4707). IEEE, doi.org/10.1109/IGARSS47720.2021.9553499,
1074 2021.

1075 Kam, S. P.: Valuing the role of living aquatic resources to rural livelihoods in multiple-use, seasonally-
1076 inundated wetlands in the Yellow River Basin of China, for improved governance, CGIAR Challenge
1077 Program on Water & Food, Colombo, Sri Lanka, <https://hdl.handle.net/10568/3859>, 2010.

1078 Kremenetski, K. V., Velichko, A. A., Borisova, O. K., MacDonald, G. M., Smith, L. C., Frey, K. E., and
1079 Orlova, L. A.: Peatlands of the Western Siberian lowlands: current knowledge on zonation, carbon
1080 content and Late Quaternary history, Quaternary Science Reviews, 22, 703-723, 2003.

1081 Kundzewicz, Z. W., Hegger, D. L. T., Matczak, P., and Driessen, P. P. J.: Opinion: Flood-risk reduction:
1082 Structural measures and diverse strategies, Proceedings of the National Academy of Sciences, 115,
1083 12321-12325, 10.1073/pnas.1818227115, 2018.

1084 Lane, C. R. and D'Amico, E.: Identification of Putative Geographically Isolated Wetlands of the
1085 Conterminous United States, JAWRA Journal of the American Water Resources Association, 52, 705-
1086 722, 10.1111/1752-1688.12421, 2016.

1087 Lane, C. R., Leibowitz, S. G., Autrey, B. C., LeDuc, S. D., and Alexander, L. C.: Hydrological, Physical,
1088 and Chemical Functions and Connectivity of Non-Floodplain Wetlands to Downstream Waters: A
1089 Review, JAWRA Journal of the American Water Resources Association, 54, 346-371, 10.1111/1752-
1090 1688.12633, 2018.

1091 Lane, C. R., Creed, I. F., Golden, H. E., Leibowitz, S. G., Mushet, D. M., Rains, M. C., Wu, Q.,
1092 D'Amico, E., Alexander, L. C., Ali, G. A., Basu, N. B., Bennett, M. G., Christensen, J. R., Cohen, M.
1093 J., Covino, T. P., DeVries, B., Hill, R. A., Jencso, K., Lang, M. W., McLaughlin, D. L., Rosenberry, D.
1094 O., Rover, J., and Vanderhoof, M. K.: Vulnerable Waters are Essential to Watershed Resilience,
1095 Ecosystems, 10.1007/s10021-021-00737-2, 2022.

1096 Lane, C. R., E. D'Amico, J. R. Christensen, H. E. Golden, Q. Wu, and A. Rajib. Global non-floodplain
1097 wetlands [dataset], https://gaftp.epa.gov/EPADDataCommons/ORD/Global_NonFloodplain_Wetlands/
1098 and <https://doi.org/10.23719/1528331>, 2023.

1099 Lehner, B. and Doll, P.: Development and validation of a global database of lakes, reservoirs and
1100 wetlands, *Journal of Hydrology*, 296, 1-22, 2004.

1101 Lehner, B. and Grill, G.: Global river hydrography and network routing: baseline data and new
1102 approaches to study the world's large river systems, *Hydrological Processes*, 27, 2171-2186,
1103 <https://doi.org/10.1002/hyp.9740>, 2013.

1104 Leibowitz, S.: Geographically Isolated Wetlands: Why We Should Keep the Term, *Wetlands*, 35, 997-
1105 1003, 10.1007/s13157-015-0691-x, 2015.

1106 Leibowitz, S. G.: Isolated wetlands and their functions: an ecological perspective, *Wetlands*, 22, 517-531,
1107 2003.

1108 Leibowitz, S. G., Hill, R. A., Creed, I. F., Compton, J. E., Golden, H. E., Weber, M. H., Rains, M. C.,
1109 Jones, J., C. E., Lee, E. H., Christensen, J. R., Bellmore, R. A., and Lane, C. R.: National hydrologic
1110 connectivity classification links wetlands with stream water quality, *Nature Water*, 1, 370-380, DOI:
1111 10.1038/s44221-023-00057-w, 2023.

1112 Liu, D., Cao, C., Chen, W., Ni, X., Tian, R., and Xing, X.: Monitoring and predicting the degradation of a
1113 semi-arid wetland due to climate change and water abstraction in the Ordos Larus relictus National
1114 Nature Reserve, China, *Geomatics, Natural Hazards and Risk*, 8, 367-383,
1115 10.1080/19475705.2016.1220024, 2017.

1116 Makungu, E. and Hughes, D. A.: Understanding and modelling the effects of wetland on the hydrology
1117 and water resources of large African river basins, *Journal of Hydrology*, 603, 127039,
1118 <https://doi.org/10.1016/j.jhydrol.2021.127039>, 2021.

1119 Martinis, S., Groth, S., Wieland, M., Knopp, L., and Rättich, M.: Towards a global seasonal and
1120 permanent reference water product from Sentinel-1/2 data for improved flood mapping, *Remote
1121 Sensing of Environment*, 278, 113077, <https://doi.org/10.1016/j.rse.2022.113077>, 2022.

1122 Marton, J. M., Creed, I. F., Lewis, D., Lane, C. R., Basu, N., Cohen, M. J., and C., C.: Geographically
1123 isolated wetlands are important biogeochemical reactors on the landscape, *BioScience*, 65, 408-418,
1124 10.1093/biosci/biv009, 2015.

1125 McCauley, L. A., Anteau, M. J., van der Burg, M. P., and Wiltermuth, M. T.: Land use and wetland
1126 drainage affect water levels and dynamics of remaining wetlands, *Ecosphere*, 6, art92, 10.1890/ES14-
1127 00494.1, 2015.

1128 McKenna, O. P., Mushet, D. M., Rosenberry, D. O., and LaBaugh, J. W.: Evidence for a climate-induced
1129 ecohydrological state shift in wetland ecosystems of the southern Prairie Pothole Region, *Climatic
1130 Change*, 145, 273-287, 10.1007/s10584-017-2097-7, 2017.

1131 McLaughlin, D. L., Kaplan, D. A., and Cohen, M. J.: A significant nexus: Geographically isolated
1132 wetlands influence landscape hydrology, *Water Resources Research*, 50, 7153-7166,
1133 10.1002/2013WR015002, 2014.

1134 Merken, R., Deboelpaep, E., Teunen, J., Saura, S., and Koedam, N.: Wetland Suitability and Connectivity
1135 for Trans-Saharan Migratory Waterbirds, *PLOS ONE*, 10, e0135445, 10.1371/journal.pone.0135445,
1136 2015.

1137 Messenger, M. L., Lehner, B., Grill, G., Nedeva, I., and Schmitt, O.: Estimating the volume and age of
1138 water stored in global lakes using a geo-statistical approach, *Nature Communications*, 7, 13603,
1139 10.1038/ncomms13603, 2016.

1140 Mudashiru, R. B., N. Sabtu, I. Abustan and W. Balogun. Flood hazard mapping methods: A review.
1141 Journal of Hydrology, 603, 126846, 2021.

1142 Mushet, D., Calhoun, A., Alexander, L., Cohen, M., DeKeyser, E., Fowler, L., Lane, C., Lang, M., Rains,
1143 M., and Walls, S.: Geographically Isolated Wetlands: Rethinking a Misnomer, Wetlands, 35, 423-431,
1144 10.1007/s13157-015-0631-9, 2015.

1145 Mushet, D. M., Alexander, L. C., Bennett, M., Schofield, K., Christensen, J. R., Ali, G., Pollard, A., Fritz,
1146 K., and Lang, M. W.: Differing Modes of Biotic Connectivity within Freshwater Ecosystem Mosaics,
1147 JAWRA Journal of the American Water Resources Association, 55, 307-317, 10.1111/1752-
1148 1688.12683, 2019.

1149 Nardi, F., Annis, A., Di Baldassarre, G., Vivoni, E. R., and Grimaldi, S.: GFPLAIN250m, a global high-
1150 resolution dataset of Earth's floodplains, Scientific Data, 6, 180309, 10.1038/sdata.2018.309, 2019.

1151 National Landcover Database (NLCD) 2019 NLCD Land Cover (CONUS), <https://www.mrlc.gov/data>,
1152 last accessed 22 December 2022.

1153 Nitzsche, K. N., Kalettka, T., Premke, K., Lischeid, G., Gessler, A., and Kayler, Z. E.: Land-use and
1154 hydroperiod affect kettle hole sediment carbon and nitrogen biogeochemistry, Science of The Total
1155 Environment, 574, 46-56, <http://dx.doi.org/10.1016/j.scitotenv.2016.09.003>, 2017.

1156 Olefeldt, D., Hovemyr, M., Kuhn, M. A., Bastviken, D., Bohn, T. J., Connolly, J., Crill, P., Euskirchen, E.
1157 S., Finkelstein, S. A., Genet, H., Grosse, G., Harris, L. I., Heffernan, L., Helbig, M., Hugelius, G.,
1158 Hutchins, R., Juutinen, S., Lara, M. J., Malhotra, A., Manies, K., McGuire, A. D., Natali, S. M.,
1159 O'Donnell, J. A., Parmentier, F. J. W., Räsänen, A., Schädel, C., Sonntag, O., Strack, M., Tank, S. E.,
1160 Treat, C., Varner, R. K., Virtanen, T., Warren, R. K., and Watts, J. D.: The Boreal–Arctic Wetland and
1161 Lake Dataset (BAWLD), Earth Syst. Sci. Data, 13, 5127-5149, 10.5194/essd-13-5127-2021, 2021.

1162 Pappenberger, F., E. Dutra, F. Wetterhall and H. L. Cloke. Deriving global flood hazard maps of fluvial
1163 floods through a physical model cascade. Hydrol. Earth Syst. Sci., 16, 11, 4143-4156, 2012.

1164 Pekel, J.-F., Cottam, A., Gorelick, N., and Belward, A. S.: High-resolution mapping of global surface
1165 water and its long-term changes, *Nature*, 540, 418-422, 10.1038/nature20584, 2016.

1166 Prigent, C., Papa, F., Aires, F., Rossow, W. B., and Matthews, E.: Global inundation dynamics inferred
1167 from multiple satellite observations, 1993–2000, *Journal of Geophysical Research: Atmospheres*, 112,
1168 <https://doi.org/10.1029/2006JD007847>, 2007.

1169 PRISM Climate Group, Parameter-elevation Regressions on Independent Slopes Model,
1170 prism.oregonstate.edu/, last accessed 22 December 2022.

1171 Rains, M. C., Leibowitz, S. G., Cohen, M. J., Creed, I. F., Golden, H. E., Jawitz, J. W., Kalla, P., Lane, C.
1172 R., Lang, M. W., and McLaughlin, D. L.: Geographically isolated wetlands are part of the hydrological
1173 landscape, *Hydrological Processes*, 30, 153-160, 10.1002/hyp.10610, 2016.

1174 Rajib, A., Golden, H. E., Lane, C. R., and Wu, Q.: Surface depression and wetland water storage
1175 improves major river basin hydrologic predictions, *Water Resources Research*, 56, e2019WR026561,
1176 <https://doi.org/10.1029/2019WR026561>, 2020.

1177 Rajib, A., Zheng, Q., Golden, H. E., Wu, Q., Lane, C. R., Christensen, J. R., Morrison, R. R., Annis, A.,
1178 and Nardi, F.: The changing face of floodplains in the Mississippi River Basin detected by a 60-year
1179 land use change dataset, *Scientific Data*, 8, 271, 10.1038/s41597-021-01048-w, 2021.

1180 Robarts, R., Zhulidov, A., and Pavlov, D.: The State of knowledge about wetlands and their future under
1181 aspects of global climate change: the situation in Russia, *Aquatic Sciences*, 75, 27-38, 10.1007/s00027-
1182 011-0230-7, 2013.

1183 Rodrigues, L. N., Sano, E. E., Steenhuis, T. S., and Passo, D. P.: Estimation of Small Reservoir Storage
1184 Capacities with Remote Sensing in the Brazilian Savannah Region, *Water Resources Management*, 26,
1185 873-882, 10.1007/s11269-011-9941-8, 2012.

1186 Rodríguez-Rodríguez, M., Aguilera, H., Guardiola-Albert, C., and Fernández-Ayuso, A.: Climate
1187 Influence Vs. Local Drivers in Surface Water-Groundwater Interactions in Eight Ponds of Doñana
1188 National Park (Southern Spain), *Wetlands*, 41, 25, 10.1007/s13157-021-01425-6, 2021.

1189 Rudari, R., Silvestro, F., Campo, L., Rebora, N., Boni, G., and Herold, C. Improvement of the global
1190 flood model for the GAR 2015. United Nations Office for Disaster Risk Reduction (UNISDR), Centro
1191 Internazionale in Monitoraggio Ambientale (CIMA), UNEP GRID-Arendal (GRID-Arendal): Geneva,
1192 Switzerland, 69, 2015.

1193 Sampson, C. C., Smith, A. M., Bates, P. D., Neal, J. C., Alfieri, L., and Freer, J. E.: A high-resolution
1194 global flood hazard model, *Water Resources Research*, 51, 7358-7381, 10.1002/2015WR016954, 2015.

1195 Samways, M. J., Deacon, C., Kietzka, G. J., Pryke, J. S., Vorster, C., and Simaika, J. P.: Value of
1196 artificial ponds for aquatic insects in drought-prone southern Africa: a review, *Biodiversity and
1197 Conservation*, 29, 3131-3150, 10.1007/s10531-020-02020-7, 2020.

1198 Sangwan, N. and Merwade, V.: A Faster and Economical Approach to Floodplain Mapping Using Soil
1199 Information, *JAWRA Journal of the American Water Resources Association*, 51, 1286-1304,
1200 10.1111/1752-1688.12306, 2015.

1201 Schofield, K. A., Alexander, L. C., Ridley, C. E., Vanderhoof, M. K., Fritz, K. M., Autrey, B. C.,
1202 DeMeester, J. E., Kepner, W. G., Lane, C. R., Leibowitz, S. G., and Pollard, A. I.: Biota Connect
1203 Aquatic Habitats throughout Freshwater Ecosystem Mosaics, *JAWRA Journal of the American Water
1204 Resources Association*, 54, 372-399, 10.1111/1752-1688.12634, 2018.

1205 Serran, J. N., Creed, I. F., Ameli, A. A., and Aldred, D. A.: Estimating rates of wetland loss using power-
1206 law functions, *Wetlands*, 38, 109-120, 10.1007/s13157-017-0960-y, 2017.

1207 Shaw, D. A., Vanderkamp, G., Conly, F. M., Pietroniro, A., and Martz, L.: The Fill–Spill Hydrology of
1208 Prairie Wetland Complexes during Drought and Deluge, *Hydrological Processes*, 26, 3147-3156,
1209 10.1002/hyp.8390, 2012.

1210 Smith, L. L., Subalusky, A. L., Atkinson, C. L., Earl, J. E., Mushet, D. M., Scott, D. E., Lance, S. L., and
1211 Johnson, S. A.: Biological Connectivity of Seasonally Poned Wetlands across Spatial and Temporal
1212 Scales, *JAWRA Journal of the American Water Resources Association*, 55, 334-353, 10.1111/1752-
1213 1688.12682, 2019.

1214 Strahler, A. N.: Quantitative analysis of watershed geomorphology, American Geophysical Union
1215 Transactions, 38, 913-920, 1957.

1216 Sullivan, S. M. P., Rains, M. C., and Rodewald, A. D.: Opinion: The proposed change to the definition of
1217 “waters of the United States” flouts sound science, Proceedings of the National Academy of Sciences,
1218 116, 11558, 10.1073/pnas.1907489116, 2019.

1219 Tayefi, V., Lane, S. N., Hardy, R. J., and Yu, D.: A comparison of one- and two-dimensional approaches
1220 to modelling flood inundation over complex upland floodplains, Hydrological Processes, 21, 3190-
1221 3202, 10.1002/hyp.6523, 2007.

1222 Tootchi, A., Jost, A., and Ducharne, A.: Multi-source global wetland maps combining surface water
1223 imagery and groundwater constraints, Earth Syst. Sci. Data, 11, 189-220, 10.5194/essd-11-189-2019,
1224 2019.

1225 Tsendbazar, N., Herold, M., Li, L., Tarko, A., de Bruin, S., Masiliunas, D., Lesiv, M., Fritz, S., Buchhorn,
1226 M., Smets, B., Van De Kerchove, R., and Duerauer, M.: Towards operational validation of annual
1227 global land cover maps, Remote Sensing of Environment, 266, 112686,
1228 <https://doi.org/10.1016/j.rse.2021.112686>, 2021.

1229 Tullos, D.: Opinion: How to achieve better flood-risk governance in the United States, Proceedings of the
1230 National Academy of Sciences, 115, 3731-3734, 10.1073/pnas.1722412115, 2018.

1231 Uden, D. R., Allen, C. R., Bishop, A. A., Grosse, R., Jorgensen, C. F., LaGrange, T. G., Stutheit, R. G.,
1232 and Vrtiska, M. P.: Predictions of future ephemeral springtime waterbird stopover habitat availability
1233 under global change, Ecosphere, 6, 1-26, 10.1890/ES15-00256.1, 2015.

1234 United States Geological Survey (USGS) National Elevation Dataset, [https://www.usgs.gov/3d-elevation-](https://www.usgs.gov/3d-elevation-program)
1235 program, last accessed 22 December 2022.

1236 United States Geological Survey (USGS) Watershed Boundary Dataset, [https://www.usgs.gov/national-](https://www.usgs.gov/national-hydrography/access-national-hydrography-products)
1237 hydrography/access-national-hydrography-products, last accessed 22 December 2022.

1238 Van Meter, K. J. and Basu, N. B.: Signatures of human impact: size distributions and spatial organization
1239 of wetlands in the Prairie Pothole landscape, *Ecological Applications*, 25, 451-465, 10.1890/14-0662.1,
1240 2015.

1241 Van Meter, K. J., Basu, N. B., Tate, E., and Wyckoff, J.: Monsoon Harvests: The Living Legacies of
1242 Rainwater Harvesting Systems in South India, *Environmental Science & Technology*, 48, 4217-4225,
1243 10.1021/es4040182, 2014.

1244 Vanderhoof, M. K. and Lane, C. R.: The potential role of very high-resolution imagery to characterise
1245 lake, wetland and stream systems across the Prairie Pothole Region, United States, *International Journal*
1246 *of Remote Sensing*, 40, 5768-5798, 10.1080/01431161.2019.1582112, 2019.

1247 Wania, R., Melton, J. R., Hodson, E. L., Poulter, B., Ringeval, B., Spahni, R., Bohn, T., Avis, C. A.,
1248 Chen, G., Eliseev, A. V., Hopcroft, P. O., Riley, W. J., Subin, Z. M., Tian, H., van Bodegom, P. M.,
1249 Kleinen, T., Yu, Z. C., Singarayer, J. S., Zürcher, S., Lettenmaier, D. P., Beerling, D. J., Denisov, S. N.,
1250 Prigent, C., Papa, F., and Kaplan, J. O.: Present state of global wetland extent and wetland methane
1251 modelling: methodology of a model inter-comparison project (WETCHIMP), *Geosci. Model Dev.*, 6,
1252 617-641, 10.5194/gmd-6-617-2013, 2013.

1253 Werner, M. G. F., Hunter, N. M., and Bates, P. D.: Identifiability of distributed floodplain roughness
1254 values in flood extent estimation, *Journal of Hydrology*, 314, 139-157,
1255 <https://doi.org/10.1016/j.jhydrol.2005.03.012>, 2005.

1256 Wickham, J., Stehman, S. V., Sorenson, D. G., Gass, L., and Dewitz, J. A.: Thematic accuracy assessment
1257 of the NLCD 2016 land cover for the conterminous United States, *Remote Sensing of Environment*,
1258 257, 112357, <https://doi.org/10.1016/j.rse.2021.112357>, 2021.

1259 Wing, O. E. J., Bates, P. D., Sampson, C. C., Smith, A. M., Johnson, K. A., and Erickson, T. A.:
1260 Validation of a 30 m resolution flood hazard model of the conterminous United States, *Water Resources*
1261 *Research*, 53, 7968-7986, 10.1002/2017WR020917, 2017.

1262 Winsemius, H. C., L. P. H. Van Beek, B. Jongman, P. J. Ward and A. Bouwman. A framework for global
1263 river flood risk assessments, *Hydrol. Earth Syst. Sci.*, 17, 5, 1871-1892, 2013.

1264 Winter, T. C.: The Vulnerability of Wetlands to Climate Change: A Hydrologic Landscape Perspective,
1265 JAWRA Journal of the American Water Resources Association, 36, 305-311, 10.1111/j.1752-
1266 1688.2000.tb04269.x, 2000.

1267 Winter, T. C., J.W. Harvey, O.L. Franke, and Alley, W. M.: Ground Water and Surface Water: A Single
1268 Resoure, U.S. Government Printing Office, Washington, DC., 1998.

1269 Woznicki, S. A., Baynes, J., Panlasigui, S., Mehaffey, M., and Neale, A.: Development of a spatially
1270 complete floodplain map of the conterminous United States using random forest, Science of The Total
1271 Environment, 647, 942-953, <https://doi.org/10.1016/j.scitotenv.2018.07.353>, 2019.

1272 Wu, Q., Lane, C. R., Wang, L., Vanderhoof, M. K., Christensen, J. R., and Liu, H.: Efficient Delineation
1273 of Nested Depression Hierarchy in Digital Elevation Models for Hydrological Analysis Using Level-Set
1274 Method, JAWRA Journal of the American Water Resources Association, 55, 354-368, 10.1111/1752-
1275 1688.12689, 2019a.

1276 Wu, Q., Lane, C. R., Li, X., Zhao, K., Zhou, Y., Clinton, N., DeVries, B., Golden, H. E., and Lang, M.
1277 W.: Integrating LiDAR data and multi-temporal aerial imagery to map wetland inundation dynamics
1278 using Google Earth Engine, Remote Sensing of Environment, 228, 1-13,
1279 <https://doi.org/10.1016/j.rse.2019.04.015>, 2019b.

1280 Xi, Y., Peng, S., Ducharne, A., Ciais, P., Gumbricht, T., Jimenez, C., Poulter, B., Prigent, C., Qiu, C.,
1281 Saunois, M., and Zhang, Z.: Gridded maps of wetlands dynamics over mid-low latitudes for 1980–2020
1282 based on TOPMODEL, Scientific Data, 9, 347, 10.1038/s41597-022-01460-w, 2022.

1283 Yamazaki, D., S. Kanae, H. Kim and T. Oki. A physically based description of floodplain inundation
1284 dynamics in a global river routing model, Water Resources Research, 47, 4, 2011.

1285 Yamazaki, D., Ikeshima, D., Sosa, J., Bates, P. D., Allen, G., and Pavelsky, T.: MERIT Hydro: A high-
1286 resolution global hydrography map based on latest topography datasets, Water Resources Research, 55,
1287 5053-5073, 10.1029/2019wr024873, 2019.

1288 Zanaga, D., Van De Kerchove, R., De Keersmaecker, W., Souverijns, N., Brockmann, C., Quast, R.,
1289 Wevers, J., Grosu, A., Paccini, A., Vergnaud, S., Cartus, O., Santoro, M., Fritz, S., Georgieva, I., Lesiv,

1290 M., Carter, S., Herold, M., Li, Linlin, Tsendbazar, N.E., Ramoïno, F., Arino, O.: ESA WorldCover 10
1291 m 2020 v100, <https://doi.org/10.5281/zenodo.5571936> 2021.

1292 Zedler, J. B. and Kercher, S.: Causes and consequences of invasive plants in wetlands: Opportunities,
1293 opportunists, and outcomes, *Critical Reviews in Plant Sciences*, 23, 431-452, 2004.

1294 Zhang, X., L. Liu, T. Zhao, X. Chen, S. Lin, J. Wang, J. Mi and W. Liu. GWL_FCS30: global 30 m
1295 wetland map with fine classification system using multi-sourced and time-series remote sensing
1296 imagery in 2020. *Earth Syst. Sci. Data* 15, 265-293, 2023.

1297 Zhu, Y., Xu, Y., Deng, X., Kwon, H., and Qin, Z.: Peatland Loss in Southeast Asia Contributing to U.S.
1298 Biofuel's Greenhouse Gas Emissions, *Environmental Science & Technology*, 10.1021/acs.est.2c01561,
1299 2022.

1300